IEEE Open Journal of
Power Electronics

Received 1 November 2023; accepted 30 November 2023. Date of publication 7 December 2023;
date of current version 26 December 2023. The review of this paper was arranged by Associate Editor Xiu Yao.

Digital Object Identifier 10.1109/OJPEL.2023.3340220

Comprehensive Overview of Power Electronics Intensive Solutions for High-Voltage Pulse Generators

YINGJIAN ZHUGE [1,2,3] (Student Member, IEEE), JUNRUI LIANG [1] (Senior Member, IEEE), MINFAN FU [1] (Senior Member, IEEE), TENG LONG [4] (Member, IEEE), AND HAOYU WANG [1] (Senior Member, IEEE)

[1]School of Information Science and Technology, ShanghaiTech University, Shanghai 201210, China
[2]Shanghai Institute of Microsystem and Information Technology, Chinese Academy of Sciences, Shanghai 200050, China
[3]University of Chinese Academy of Sciences, Beijing 100049, China
[4]Electrical Engineering Division, Department of Engineering, University of Cambridge, CB3 0FA Cambridge, U.K.

CORRESPONDING AUTHOR: HAOYU WANG (e-mail: wanghy@shanghaitech.edu.cn)

This work was supported by the National Natural Science Foundation of China under Grant 52077140.

ABSTRACT With the advancements in power semiconductors and converters, power electronics based high-voltage pulse generators (HVPG) have emerged due to their advantages of high repetition rate, flexible control, long lifetime, and compact size. However, there is a lack of comprehensive literature review on recent advances in power electronics intensive HVPG technologies. To fill this gap, we present a systematic review on HVPGs. First, HVPGs are classified into different types based on their mechanisms. Each type along with its basic circuits and modifications are introduced. Then, the characteristics, advantages, and disadvantages of these topologies are summarized. Furthermore, the potential applications of HVPGs are explored. The performance of pulse generators mentioned in the literature and commercial products is listed. Finally, future trends and technical challenges in HVPG design and development are discussed. This paper provides a clear understanding of HVPGs and the inspiration of topologies developments to meet the specific requirements. Current state and potential future directions are discussed and summarized to facilitate evolvements in HVPG technology.

INDEX TERMS High voltage, power electronics, pulse generator, pulsed power supply.

I. INTRODUCTION

Pulsed power technology involves the accumulation of energy over an extended duration, followed by its rapid discharge within a significantly shorter time frame. This results in a pulse capable of delivering substantial power to a designated target. High-voltage pulse generators (HVPG) find extensive applications in emerging applications, such as ultra-wideband radiation, material modification, cancer treatment, sterilization, and fusion systems. These applications continue to stimulate active research and development [1], [2], [3], [4], [5].

Compared with DC and AC power sources, pulsed power sources offer numerous advantages. For instance, they facilitate the formation of a more uniform and stable discharge in dielectric barrier discharge [6]. They can also improve the efficiency and quality of some processes that involves material modification [7]. Moreover, pulsed power sources enable precise control over the output pulses, which is beneficial in medical therapies such as electroporation, where a specific electric field is required [8]. Therefore, the versatility and superior performance of pulsed power sources make them an optimal choice for a wide range of applications.

There are primarily two fundamental approaches to generate high-voltage (HV) pulses, differing in their methods of energy storage [9]. One approach involves storing electric field energy in capacitors, which is followed by energy transfer to the load. The other approach relies on the accumulation of magnetic field energy in inductors, which is then transferred to the load, as illustrated in Fig. 1.

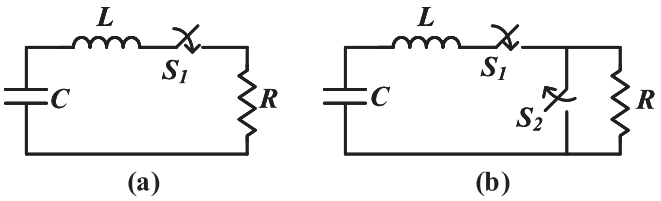

FIGURE 1. Basic approach to generate pulses. (a) capacitive energy storage; (b) inductive energy storage [9].

In Fig. 1(a), capacitor C is initially precharged to a specific voltage and discharged through stray inductance L when switch S_1 is closed. On the other hand, circuit in Fig. 1(b) operates based on a different principle. Initially, switch S_2 is closed, allowing the energy stored in capacitor C to be transferred to inductor L. Once the current reaches its maximum value, switch S_2 is opened, causing the energy to be transferred from the inductor L to the load R.

Based on their operation principle and the devices used, pulse generators can be broadly categorized into two types: classical pulse generators and power electronics based pulse generators. In classical pulse generators, the most commonly employed switches are spark gap switches and mechanical switches. Although these switches can handle high levels of voltage and current, they lack sufficient power density and compactness, and their pulse repetition frequency is limited [10]. Such pulse generators are typically utilized in large-scale facilities that require particularly high levels of voltage and current with utmost reliability.

A feasible approach to enhance performance is through the utilization of power electronics. Power semiconductors can operate at much higher repetition rates with low jitter and fast rise time [11], [12]. Additionally, high power density is desirable to meet space constraints. The use of power semiconductors, particularly wide bandgap semiconductors, such as silicon carbide (SiC) and gallium nitride (GaN) MOSFETs, holds promise for increasing power density [13]. However, the output performance is limited by heat transfer, and reliability is closely tied to the characteristics of the semiconductor material, which are temperature-dependent. Therefore, effective thermal management is essential [14], [15], [16]. Moreover, for safety purposes, galvanic isolation is required.

To cater to a wide range of applications, a pulse generator should possess flexibility and controllability, enabling it to generate pulses with arbitrary waveforms [17], [18]. In certain specific applications like cancer treatment, the capability for bipolar operation is also crucial [19], [20]. Traditionally, generating bipolar pulses involves utilizing an H-bridge module, which requires high-voltage switches. However, if it is possible to achieve bipolar pulse generation through topological modifications without compromising the performance of the output pulse, this can lead to cost reduction and improved compactness.

In summary, depending on the specific applications, a pulse generator requires some or all of the following design requirements [10], [11], [12], [13], [14], [15], [16], [17], [18], [19], [20]:

1) High voltage and current rating.
2) High pulse repetition frequency.
3) Fast rise time.
4) High power density.
5) High reliability.
6) Galvanic isolation.
7) High flexibility and controllability.
8) Bipolar operation.

Significant efforts have been dedicated to the evolution of HVPG topologies in the past decade. In [21], a historical account of the development of Marx circuit and synchronous isolated driving techniques for switches is provided, it solely focuses on Marx type generators. In [9], a review of research on solid-state generators based on inductive energy storage and semiconductor opening switches (SOS) is presented, while in [22], pulse generators for water treatment applications are reviewed. However, there is still a lack of a comprehensive overview encompassing the various power electronics intensive HVPG topologies for various applications. Therefore, the objective of this study is to bridge this gap by presenting an updated review of recent advancements in HVPG topologies. Additionally, we explore applications, technical challenges, and future trends, which can inspire the development of new HVPG topologies to meet diverse requirements.

In this paper, we focus on discussing and summarizing recent literature that report the developments of high-voltage pulse generators over the past decade. The structure of this paper is as follows: Firstly, the classical HVPGs and their recent advancements are reviewed. Next, Section III focuses on solid-state HVPGs based on power electronics. It is important to note that the topologies presented in Section II and Section III can be combined. Section IV showcases typical applications that utilize HVPGs. The performance of some pulse generators mentioned in the literature and commercial products is also listed. Section V presents the future research challenges and directions of HVPGs. Finally, we draw our conclusion in Section VI.

II. CLASSIC HIGH VOLTAGE PULSE GENERATOR

The fundamental operation of pulse generators involves storing energy in capacitors or inductors, and subsequently discharging them in series to generate the desired high-voltage pulse. High-voltage pulse generators can be classified into two main categories: classical pulse generators, and power electronics based pulse generators, as illustrated in Fig. 2.

The classical pulse generator can be further divided into several subcategories, namely: Marx generators, Pulse Forming Networks (PFN), Pulse Forming Lines (PFL) and Blumlein Lines (BL), Tesla Transformer, and Magnetic Pulse Compression (MPC).

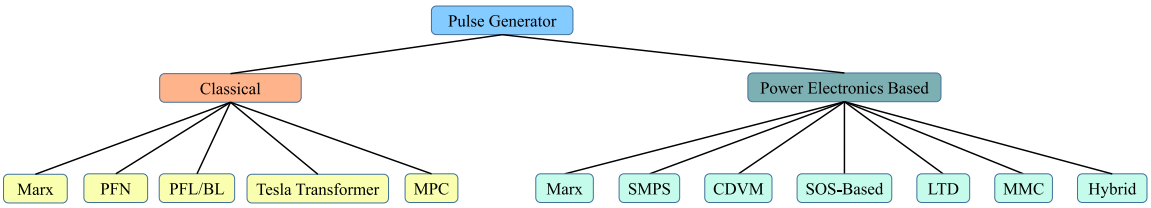

FIGURE 2. Classification of high-voltage pulse generators.

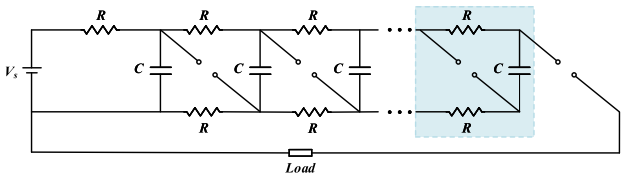

FIGURE 3. Circuit diagram of classical Marx generator.

A. MARX GENERATOR

Marx generator, first invented by Erwin Marx in 1925, has been extensively investigated to generate high-voltage pulses. Since its inception, the Marx generator has remained a popular topology for pulse generation. The basic circuit diagram of a Marx generator is shown in Fig. 3.

The operational principle is as follows: initially, the spark gap switches are not triggered, and N energy-storing capacitors C are charged in parallel from a relatively low voltage power supply through the charging resistors R. Subsequently, all spark gap switches are sequentially conducted. As a result, all the capacitors are connected in series, generating a high-voltage pulse across the load. In ideal conditions with no losses, the amplitude of pulse is the product of the number of capacitors N and the input voltage V_s.

Spark gap switches are commonly utilized as switches in Marx generator due to their high-power capacity and high di/dt [23]. However, spark gap switches possess certain drawbacks. Firstly, they tend to be bulky, vulnerable and not suitable for high repetition frequency applications. Moreover, adjusting pulse width of the pulse can be challenging with spark gap switches.

Marx generators with spark gap switches are generally utilized in high-power applications, whose recent researches focus on miniaturization, compactness and pulse shaping. In [24], based on the Fourier theory, capacitors with different capacity are used to generate near-square pulses. In [25], a coaxial integrated structure is employed to enhance compactness. In [26], the research on key technologies and essential components contributes to the development and application of compact and repetitive Marx generators, promising their miniaturization.

B. PULSE FORMING NETWORKS

Marx generators are commonly used for generating high-voltage pulses, but their output pulses exhibit an exponential

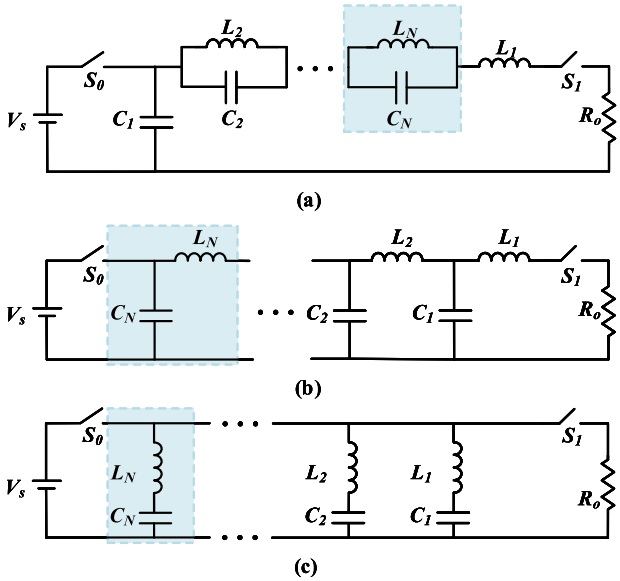

FIGURE 4. Circuit diagram of pulse forming networks (a) Type-A PFN; (b) Type-B PFN; (c) Type-C PFN [27].

shape due to the nature of the RC network. However, in certain applications, a rectangular pulse shape is required. To achieve this, PFNs consisting of inductors and capacitors are typically employed.

As shown in Fig. 4, PFNs can be classified into three basic topologies: Type A, Type B, and Type C, as described in [27]. The capacitors and inductors in Type A or Type B PFN have equal L_i and C_i,

For a typical Guillemin Type C network depicted in Fig. 4(c), the current flow over the load R_0 is the sum of each LC section [28]. The relationships between each cell to generate a square current waveform can be derived based on the Fourier series expression:

$$C_n = \frac{1}{(2n-1)^2} C_1 \tag{1}$$

$$L_n = L_1. \tag{2}$$

PFN topologies are preferred due to their advantages of limited stored energy and a relatively simple structure. However, they also have notable drawbacks. Firstly, the output voltage of a PFN is half of the DC charging voltage when connecting to a matched load. Additionally, these topologies tend to

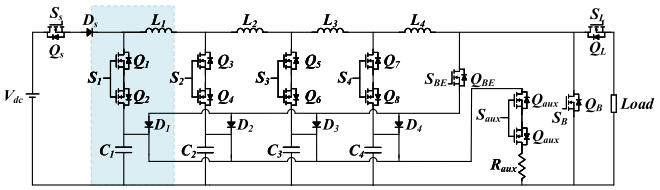

FIGURE 5. PFN-Boost circuit [31].

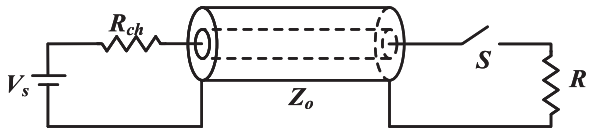

FIGURE 6. Circuit diagram of transmission line.

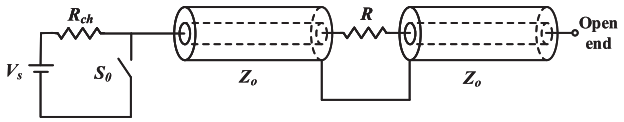

FIGURE 7. Circuit diagram of Blumlein Lines.

exhibit poor pulse quality, a constant pulse width, and a limited range of load variation.

Efforts have been made to address the aforementioned challenges. One straightforward approach to increase the output voltage is using transformer [29]. However, transformers are usually bulky and costly. This inspires the idea of making a composition of PFN and other voltage multiplier topologies, such as Marx circuit [30], and boost converter [31], as illustrated in Fig. 5.

C. PULSE FORMING LINES AND BLUMLEIN LINES

Similar to PFNs, pulse forming lines are also extensively employed for generating 1 to 100 ns rectangular pulses [32]. The schematic of a transmission line (TL) is illustrated in Fig. 6. The load impedance (R) is equal to the characteristic impedance (Z_0) of the PFL, and the output voltage is half of the input voltage.

Blumlein Lines are designed to achieve output voltage equal to the input voltage, as depicted in Fig. 7. In this configuration, the load is connected in series between the paired transmission lines, which the impedance of the load is twice the characteristic impedance of each transmission line ($R = 2Z_0$).

To achieve higher voltage levels, module stacking is a commonly employed method. In this regard, a multistage Blumlein lines and Transmission Line Transformer (TLT) stacking technique is proposed, as illustrated in Fig. 8. This approach enables the generation of pulses with high voltage, adjustable polarity, fast rise and fall time, and narrow pulse width. Additionally, the output parameters can be easily adjusted by manipulating the control signal of the switches [33], [34].

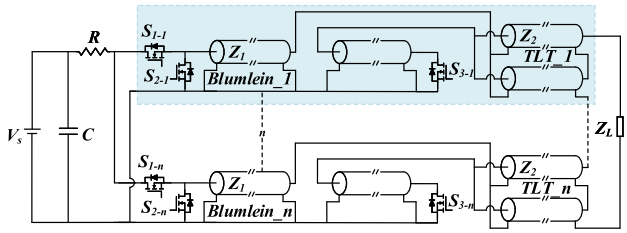

FIGURE 8. Nanosecond pulse generator based on Blumlein and TLT [34].

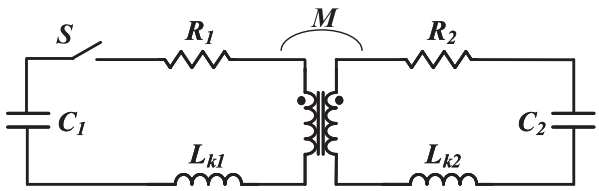

FIGURE 9. Double resonance circuit of Tesla transformer [37].

Blumlein lines are capable of generating nanosecond rectangular pulses in a simple and efficient manner. However, traditional Blumlein Lines that utilize coaxial cable transmission lines face challenges in adjusting the pulse polarity and duration flexibly. They also have the disadvantage of occupying a large space. Many improvements are proposed to address these drawbacks. In [35], a multilayered PCB-based Blumlein strip transmission line is utilized to reduce space occupancy, while adjustable pulse width and output impedance can be implemented through multistage series-parallel structure.

D. TESLA TRANSFORMER-BASED CIRCUIT

Pulse Transformer is another method to achieve high-voltage pulses. There are commonly two groups: air-core Tesla transformer and magnetic-core transformer [36]. The typical air-core Tesla transformer consists of two coupled resonant loops with the identical intrinsic resonant frequencies or only minor difference, as shown in Fig. 9.

Since the air-core Tesla transformer eliminate the magnetic core and transfer energy through the magnetic coupling of the air, its overall weight and volume can be greatly reduced, and it avoids magnetic saturation and frequency limitation, which enables long lifetime and high repetition rate. However, the main issue is that the coupling coefficient is generally less than 0.8, which limits the efficiency and transformation ratio [37].

To improve the coupling efficient and transmission efficiency, open-magnetic-core Tesla transformer was firstly constructed in Russia. Two windings are mounted in the PFL, and the inner and outer cylinders of PFL are replaced by open-magnetic core. The representative generators are Sinus-series [38] and RADAN [39]. Recent development about open-magnetic-core Tesla transformer-based generators include: multi-wire-layered secondary winding [40], [41], copper-titanium-composite primary wingding [42], magnetically insulation [43], low-impedance PFL [44], film-rolled coaxial PFL [45], PFN [46], [47], bipolar modulation [48].

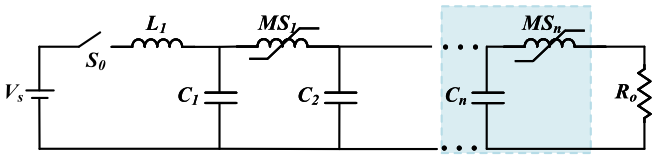

FIGURE 10. Circuit diagram of magnetic pulse compression.

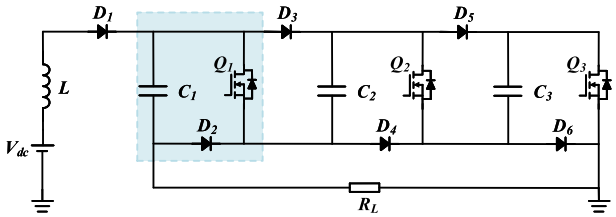

FIGURE 11. Typical solid-state Marx generator [61].

E. MAGNETIC PULSE COMPRESSION

Magnetic Pulse Compression systems are also widely used in many systems due to their numerous advantages, including high repetition rate, high reliability, long service life and high power capability [49], [50], [51]. The n-stage MPC circuit is depicted in Fig. 10, where each stage consists of a capacitor and a magnetic switch.

In the MPC circuit, when the capacitor starts to be charged, the magnetic switch has a large inductance. Energy transfer between two adjacent capacitors occurs when the potential of the former one reaches V that leads to magnetic switch saturation. The switch with a large inductance saturates due to the leakage current flowing through the coil.

When the first magnetic switch reaches saturation, the core inductance decreases to its initial value of $1/\mu$. This change causes the switch MS_1 to close, allowing energy transfer from C_1 to C_2. Similarly, magnetic switches in the subsequent stages of the MPC circuit further compress the pulse rise time and amplify the current [52].

Despite their numerous advantages, magnetic switches still face certain limitations, such as core losses, challenges in instantaneous control, and the presence of arcs caused by residual energy. Core losses are directly related to the volumes of the cores. Minimizing the core volumes can effectively reduce overall costs, size, and weight of the generator. In [53], theoretical analyses are presented, along with the design and performance optimization methods. By regulating the reversed currents in the windings, the saturation inductance can be reduced to a level below its structural inductance, resulting in a magnetic switch with ultra-low saturation inductance [54]. The reset current control method is introduced to enhance efficiency under variable load and pulse frequency conditions [55], [56].

In addition to improving the performance of magnetic switches, MPC can be combined with other topologies to enhance pulse performance. For instance, in [57], a single-stage MPC is used in conjunction with a Marx circuit to further reduce the rise time. Additionally, the peaking capacitor in the MPC can be replaced with a PFL or BL, which offers alternative means to improve the pulse characteristics.

III. POWER ELECTRONICS BASED HIGH VOLTAGE PULSE GENERATOR

With the advancements in power semiconductors and converters, high-voltage pulse generators based on power electronics are emerging. These solid-state pulse generators offer advantages such as high reliability, high repetition rate, long lifetime, and compact size. As a result, they have garnered increasing research attention [58], [59], [60].

The existing power electronics based pulse generators can be categorized into seven main groups: Marx generators, switched-mode power supplies (SMPS), capacitor-diode voltage multipliers (CDVM), semiconductor opening switches (SOS)-based pulse generators, linear transformer driver (LTD), modular multilevel converters (MMC), and hybrid generators.

A. MARX GENERATOR

Solid-state Marx generators have been investigated by emulating the classical Marx generators. The advancement of semiconductor devices has propelled the development of solid-state Marx generators. The key concept is to replace spark gap switch with power electronic switch, such as IGBTs, MOSFETs, and avalanche transistors (ATs). An example of a solid-state Marx generator utilizing MOSFETs is illustrated in Fig. 11 [61].

For solid-state Marx generators, a key challenge is the requirement for high voltage isolation in the driving circuit of the switches, given the varying potentials at which these switches operate during the discharge phase. Commonly employed isolation methods include: 1) use an isolated power supply for each driving circuit; 2) leverage a transformer for driving signal provision. However, each method comes with its drawbacks. Using isolated power supply can lead to issues of miniaturization and increased cost, whereas implementing a driving transformer can compromise the rising edge characteristics of the driving signal, thereby affecting the synchronization between stages.

Research has been undertaken to address these problems in the driving circuit of solid-state Marx generators. One intuitive solution is to connect several switches in series to form a single switch, which directly reduces the required number of driving transformers. As depicted in Fig. 12, multiple MOSFETs are employed to create a self-triggering high-voltage switch in series directly. Moreover, these modules are harnessed to create a Marx circuit, enabling the attainment of a higher voltage pulse [13].

An alternative method involves designing a self-triggering topology. As Fig. 13 indicates, the primary circuit follows the classical Marx configuration. However, it requires only a single gate drive signal for the lowest stage, eliminating the need for high voltage isolation. The remaining stages employ a high

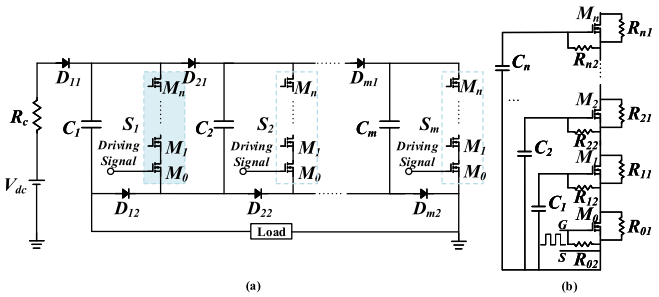

FIGURE 12. Marx generator employing the SiC MOSFETs module. (a)Marx-type pulse generator employing this module as the main switch. (b)series-connected MOSFETs module [13].

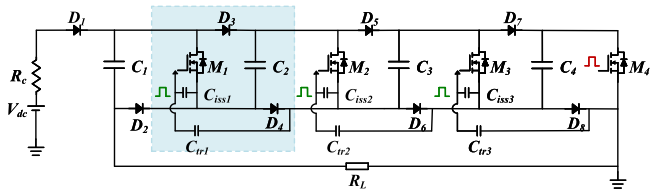

FIGURE 13. Self-triggering Marx generator [62].

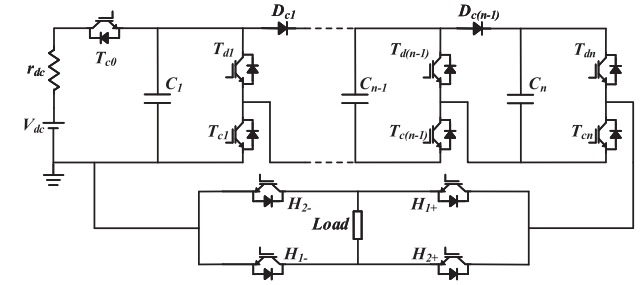

FIGURE 14. Bipolar Marx generator with H-bridge [63].

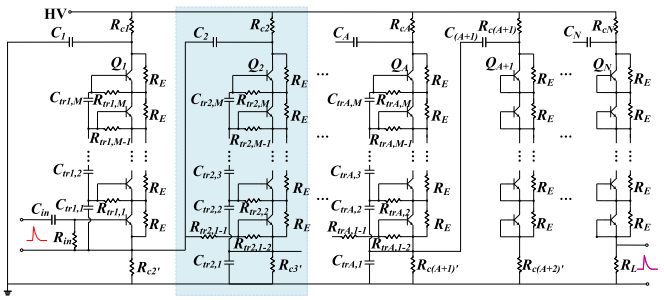

FIGURE 15. Modified AT-based Marx generator with auxiliary triggering topology [69].

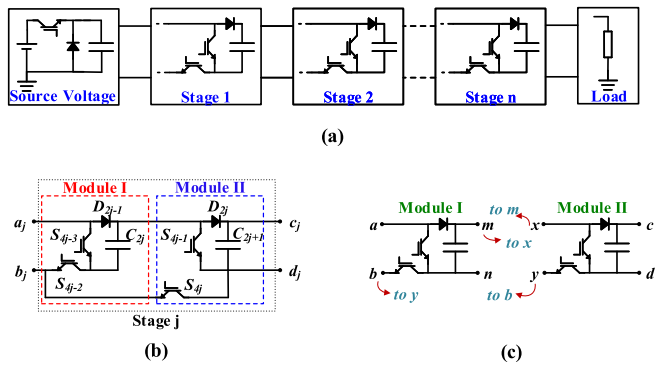

FIGURE 16. Modified high-voltage pulse generator based on switched-capacitor units. (a) N-stage prototype. (b) One stage. (c) Two submodules and their connections [70].

potential-energy-gaining technology, utilizing the interstage capacitors to trigger the other MOSFETs sequentially [62].

While these topologies can generate unipolar pulses, there are certain applications that necessitates bipolar pulses. A fundamental method to achieve this is to incorporate an H-bridge on the load side, as illustrated in Fig. 14. The Marx generator is in series with an H-bridge to output pulses of varying polarities [63]. Furthermore, various configurations of the Marx generator can be utilized to generate bipolar high-voltage pulses without the need for an H-bridge. These configurations include the double power charging Marx generator [64], cascade of positive and negative Marx generator [65], and dual Marx generator [66].

Apart from the commonly utilized IGBTs and MOSFETs, avalanche transistors have found extensive use in generating nanosecond and sub-nanosecond pulses due to their fast switching speed [67]. However, in typical AT-based Marx circuit, transistors in the first several stages are prone to failure due to an insufficient overvoltage ramp and a deficiency in transient current. Further, the initial charge carriers generated by a low overvoltage ramp are inadequate to reliably drive the barrier region into the avalanche state, thereby significantly limiting the adjustable range of the output voltage [68].

To address these issues, a modified circuit that utilizes base-triggering method is proposed, as shown in Fig. 15. A shunting resistor is introduced to create an inner triggering loop with a trigger capacitor for each transistor in the first several stages. The induced additional base current alters the switched-on modes, and promotes reliable conduction even in the presence of an insufficient overvoltage ramp. This modification significantly extends the operational voltage range [69].

The voltage gain of a classical Marx generator is proportional to the number of capacitors, resulting in a V/C ratio close to 1. To attain a higher output voltage, more capacitors are required, which largely influences the size and energy density. Consequently, it is essential to reduce the number of capacitors, thus increasing the V/C ratio.

As depicted in Fig. 16, a switched-capacitor converter is developed in [70]. The V/C ratio is elevated to 2 with a slight modification to the Marx circuit. Each capacitor is charged in series by the capacitors in previous stages in series to reach a higher voltage. Therefore, the higher output voltage can be obtained. However, there is still remaining potential during the discharging process.

In summary, Table 1 provides a straightforward comparison among various solid-state Marx generators, all sharing

TABLE 1. Comparison of Solid-State Marx Generators

Topology	Switch Type	Number of Switches	Number of Diodes	Number of Main Capacitors	Number of Drivers	Main Switch Voltage	Output Voltage Gain
Classic Marx Generator	MOSFET	k	$2k$	k	k	U_{dc}	k
[13]	MOSFET	mk	$2k$	k	k	$\frac{1}{m}U_{dc}$	k
[62]	MOSFET	k	$2k$	k	1	U_{dc}	k
[69]	Avalanche Transistor	mk	0	k	1	$\frac{1}{m}U_{dc}$	k
[70]	IGBT	$4k_0+1$	$2k_0$	$2k_0+1$	$2k_0+2$	$(2k-1)U_{dc}$	k

* $k_0 = log_2(\frac{k+2}{3})$
** m is the number of switches in series.

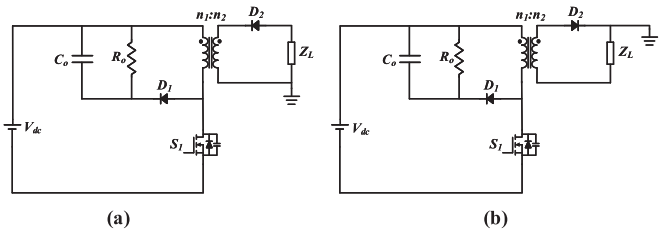

FIGURE 17. Schematic of SMPS. (a) Flyback-type topology; (b) Forward-type topology [71].

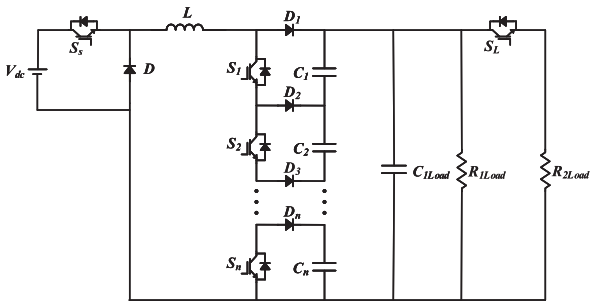

FIGURE 18. Buck-boost-converter-based pulse generator with multi switch-diode-capacitor units [74].

identical input and output voltages. The table lists the number of components (switches, diodes, capacitors, and drivers) and compares the voltage stresses of switches across different topologies. Compared with classical Marx generator, these work have achieved lower voltage stresses of switches, lower components count, and improved V/C ratio.

B. SWITCHED-MODE POWER SUPPLY

Switched-mode power supplies are often employed to generate high voltage pulses, with a particular focus on DC/DC converters due to their step-up capabilities. This presents an alternative to the use of high-voltage modulators with series-connected semiconductor switches. The fundamental topology involves connecting a high-voltage switch to the converters to generate a pulse through chopping. The most commonly used topologies include Flyback, Buck-Boost, and Boost converters.

In [71], two topologies are discussed: flyback and isolated forward converters with a step-up transformer to further increase the output voltage, as depicted in Fig. 17. Compared with classical flyback and forward converters, the output filter is omitted. The RCD voltage clamp circuit, connected to the transformer's primary winding, is used to demagnetize the transformer and to reduce voltage spike.

The boost-derived ringing circuit is proposed in [72]. This configuration allows for enhanced efficiency and high voltage gain. However, the associated semiconductor devices need to

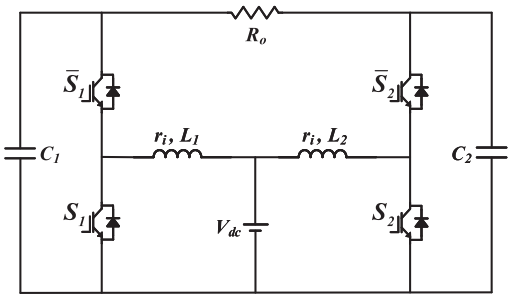

FIGURE 19. Boost-inverter-based pulse generator [75].

be rated at the high-voltage level, and the pulse periodic time is constrained. To mitigate these limitations, several multi-module topologies — specifically, interleaved, stacked, and stacked-interleaved — have been suggested [73].

In [74], a pulse generator based on the buck-boost converter is proposed for plasma applications. Additionally, a series of switch-capacitor units is used to provide high voltage gain with a high voltage stress dv/dt. As a result, the sum of these voltages appears at the output terminal.

The topologies mentioned earlier can only generate unipolar pulses unless an additional H-stage is employed. In [75], a boost-inverter-derived bipolar high-voltage pulse generator is proposed. This system, illustrated in Fig. 19, comprises two

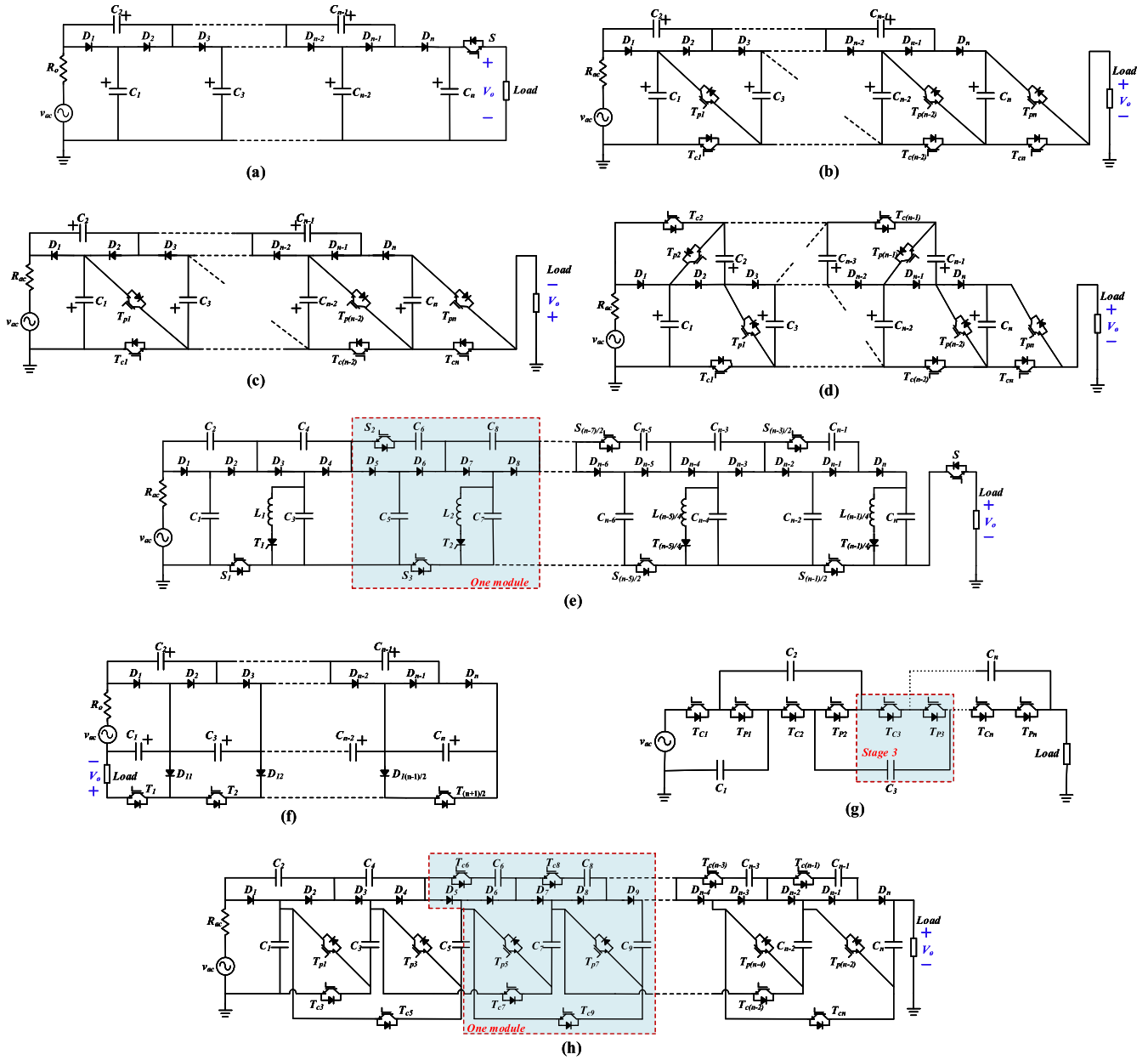

FIGURE 20. Pulse generator based on CDVM. (a) Traditional CDVM topology. (b) Positive series-parallel voltage multiplier (SPVM) topology [76]. (c) Negative SPVM topology [76]. (d) Parallel-parallel voltage multiplier (PPVM) topology [77]. (e) Modified topology of the circuit in (a) [17]. (f) Series-series voltage multiplier (SSVM) topology [77]. (g) Modified topology of the circuit in (f) [78]. (h) Combination of SSVM and SPVM topology [79].

bidirectional boost converters with the load differentially connected between the output terminals. Compared with H-bridge methods, this system only requires two high-voltage switches, which favorably impacts system cost and complexity.

C. CAPACITOR-DIODE VOLTAGE MULTIPLIER

Capacitor-diode voltage multipliers are widely used in many circuit designs and industrial applications, due to their simplicity, high reliability, and high efficiency. Generally, CDVM topologies operate by charging a set of capacitors with a low-voltage AC source, incrementally boosting the input voltage, and producing high voltage across the load via a high-voltage chopping switch, which governs the repetition rate and pulse width. Fig. 20 depicts a typical voltage multiplier converter and its enhanced topologies.

The basic CDVM topology is shown in Fig. 20(a). During pulse generation, only the last capacitor discharges. An attractive idea is that if each bottom capacitor is connected in series, the resulting voltage would be the sum of each capacitor voltage. Therefore, numerous modified topologies have been derived from the typical CDVM.

Fig. 20(b) illustrates a series-parallel voltage multiplier (SPVM) proposed in [76]. During the charging mode, switches T_{ci} are turned on, and switches T_{pi} are turned off.

TABLE 2. Comparison Between Different CDVM Topologies Based on the Elements and Performance

Topology	Voltage Gain	No. of Switches	Switch Voltage	No. of Diodes	Diode Voltage	No. of Capacitors	Capacitor Voltage
Fig. 20(b)	$(\frac{n+1}{2})^2$	n+1	1, 3, 5,..., n V_{in}	n	n V_{in} (D_n) 2 V_{in}	n	2 V_{in} (top) 1, 3, 5,..., n V_{in} (bottom)
Fig. 20(c)	$(\frac{n+1}{2})^2$	n+1	1, 3, 5,..., n V_{in}	n	n V_{in} (D_n) 2 V_{in}	n	2 V_{in} (top) 1, 3, 5,..., n V_{in} (bottom)
Fig. 20(d)	$\frac{n(n+1)}{2}$	$2n$	2, 3, 4,..., 2n-3 V_{in}	n	2,2,3,4,...,n V_{in}	n	2, 4, 6,..., (n-1) V_{in} (top) 1, 3, 5,..., n V_{in} (bottom)
Fig. 20(e)	$(\frac{n+1}{2})^2$	$\frac{n+1}{2}$	4, 8, 12,..., 2n-2 V_{in}	n	2 V_{in}	n	1,3,5,...,n V_{in}
Fig. 20(f)	n	$\frac{n+1}{2}$	1 V_{in} (T_1) 2 V_{in}	$n+\frac{n-1}{2}$	2 V_{in}	n	1 V_{in}(C_1) 2 V_{in}
Fig. 20(g)	$2n-1$	$2n$	1 V_{in} (T_{Cn}, T_{Pn}) 2 V_{in}	$2n$	2 V_{in}	n	1 V_{in} (C_1) 2 V_{in}
Fig. 20(h)	$2n-2$	$\frac{n-1}{2}+n-3$	1, 2, 3, 4 V_{in}	n	2 V_{in}	n	2 V_{in} (top) 1, 3, 4, 4,..., 4 V_{in} (bottom)

In the positive half cycle, odd diodes are in forward bias and bottom capacitors charged; In the negative half cycle, the even diodes are forward-biased and the top capacitors are charged. During the discharging mode, switches T_{ci} are turned off and switches T_{pi} are turned on, causing the odd capacitors to be discharged in series. If the polarities of all semiconductors are reversed, as shown in Fig. 20(c), the generator delivers negative pulses.

However, this circuit design causes each bottom capacitor to be charged with the input voltage multiplied by an increasingly odd factor, leading to successively increasing voltage ratings for T_{ci} and T_{pi} at each stage. In addition, each switch conducts different currents for charging and pulse generation. Consequently, standardization is compromised. Furthermore, switch triggering poses a significant challenge due to the various potentials of each switch.

An alternative topology can be achieved by adding the voltages of each top capacitor (with an even index) to the output to yield a higher voltage, named the parallel-parallel voltage multiplier (PPVM), as shown in Fig. 20(d). Compared with SPVM, the output voltage increases significantly, along with the increases in the number of switches [77].

In [17], combination of CDVM with resonant converter is presented to generate high-voltage wide pulses combined with narrow pulses, as shown in Fig. 20(e). Inductors are connected to the capacitors through switches to form the resonant circuits to change the polarities of capacitor voltages.

As illustrated in Fig. 20(f), in [77], another approach is proposed to improve the modularity. The blocking voltages of the switches in each stage are constant and equal to $2V_{in}$ except S_1.

In [78], a modified topology is proposed to utilize even capacitors during the discharge mode, as illustrated in Fig. 20(g). The circuit employs a modular configuration and the voltage across all components is equal to $2V_{in}$, except for T_{cn} and T_{pn}. During the discharge mode, switches T_{ci} are turned off and switches T_{pi} are turned on, connecting all capacitors in series and enabling them to be discharged.

As previously discussed, the combination of SPVM and PPVM appears to be a promising solution to their stated problems and combines their respective benefits, as described in [79]. This structure is modular and can be expanded to more stages without increasing the voltage rating of the devices, as depicted in Fig. 20(h).

It is important to note that achieving the maximum voltage in CDVM-based generators requires multiple cycles to charge each capacitor. Therefore, these generators may not be suitable for nanosecond or subnanosecond applications. Table 2 presents a simple comparison of the mentioned topologies based on the number of elements and their performance.

D. SEMICONDUCTOR OPENING SWITCH-BASED CIRCUIT

Traditional semiconductor switches like IGBTs and MOSFETs face challenges in meeting the fundamental requirements of high current decreasing rate (di/dt) and withstand voltage. These limitations have driven the development of semiconductor opening switches, such as drift step recovery diodes (DSRD) or the other devices with

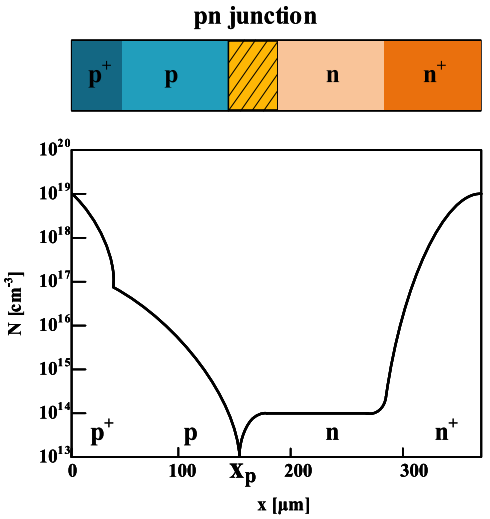

FIGURE 21. Typical p^+-p-n-n^+ structure of an SOS diode.

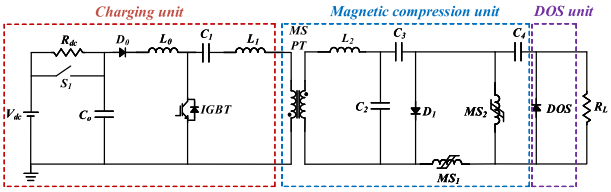

FIGURE 22. DOS-based high voltage pulse generator [87].

similar characteristics. These devices exhibit high current density, high operating voltage, and short current cutoff time [80], [81], [82], [83], [84]. The primary mechanism behind their operation involves carrier accumulation through forward current and extraction through reverse current.

In 1983, Grekhov proposed and implemented a high-current operating mode for a p^+-n-n^+ silicon diode structure known as the DSRD. These diodes showcase a cutoff current density of 200 A/cm^2, a current cutoff time of 2 ns, and an operating voltage of 1 kV [85]. The principle of operation for DSRDs is detailed in [86]. In 1990 s, the Semiconductor Opening Switch (SOS) effect was discovered, which involves nanosecond cutoffs of superdense currents in semiconductors. This effect occurs in p^+-p-n-n^+ silicon diode structures with pumping times in the range of hundreds of nanoseconds and reverse current densities ranging from a few to tens of kiloamperes per square centimeter. Further research on this effect has laid the foundation for the development of superpower SOS devices, which employ a p^+-p-n-n^+ silicon diode structure (shown in Fig. 21). These devices achieve current density several orders of magnitude higher than DSRDs.

In [87], Diode Opening Switch (DOS) is developed, which operates based on similar principle as SOS and DSRD. DOS has a basic structure as a PIN diode. As depicted in Fig. 22, the generator utilizing DOS is composed of three units: charging unit, magnetic compression unit, and DOS unit. The MPC unit serves to increase the voltage amplitude, compress the

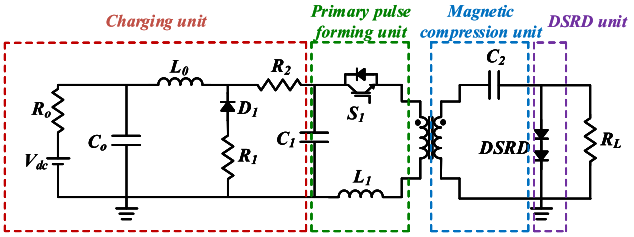

FIGURE 23. DSRD-based saturable pulse transformer type pulse generator [88].

pulse width and the rise time, and provide the forward and reverse pumping currents for the DOS. During operation, the forward pumping circuit ($C_3 - C_2 - MS_1 - DOS - C_4$) is turned on, supplying the DOS unit with a forward pumping current, resulting in the accumulation of a large number of carriers. Subsequently, the reverse pumping circuit ($C_4 - DOS - MS_2$) is activated, causing the reverse current and accumulated carriers extracted. Once the carriers are depleted, the current is cut off, and the current through the loop inductance is rapidly transferred to the load, generating a high-amplitude pulse with fast rise time.

As illustrated in Fig. 23, the generator is composed of a charging unit, a primary pulse forming unit, a magnetic pulse compression unit, and a DSRD unit. The operational mode is similar to the circuit discussed earlier. It has the capability to operate steadily at a frequency of 100 kHz with a peak voltage of nearly 30 kV, or at a frequency of 25 kHz with a peak voltage of 140 kV [88].

These new type of semiconductor pulsed power switches, such as DSRD and SOS, can achieve unique advantages. These include ns-level jitter and delay, high response speed, high power capacity, large dynamic range, and simple structure. However, the high cost and the relative immaturity of the technology present significant challenges, which currently limit their widespread application.

E. LINEAR TRANSFORMER DRIVER

Linear Transformer Driver is an approach to enhance the pulse amplitude. The basic structure of LTD is a pulse transformer, where the turn ratio is 1. The typical LTD consists of several low-power pulses connected in parallel to form a high-power pulse. All modules are grounded, thereby reducing the complexity of the power supply and significantly enhancing modularity. Additionally, for an LTD system, different modules can be switched at different timings, which means pulse shape flexibility [89].

The pulsed-power generators based on LTD started with large devices where gas switches are used, aiming at potential applications to inertial fusion drivers [90]. On the other hand, the solid-state LTD based on semiconductor switches has received much attention in industrial applications due to high repetition rate and turning-off ability [91], [92]. In [89], the LTD system consists of 30 modules each containing 24 unit circuits, which can generate a pulse, with a voltage

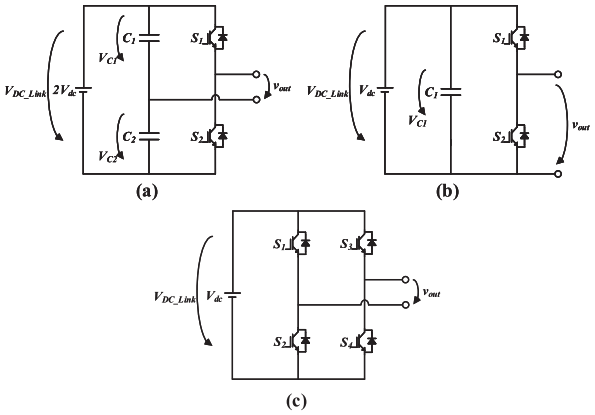

FIGURE 24. Basic submodules of MMC. (a) Symmetrical half-bridge (HB); (b) Asymmetrical half-bridge; (c) H-bridge [93].

amplitude of 30 kV, a peak current of 250 A, and pulse width adjustable in the range of 50-170 ns. Moreover, by controlling the switching signals, precise waveform control can be realized.

The conventional unipolar LTD often uses a multi-branch parallel discharge structure, but it requires an active reset circuit due to the saturation of magnetic core. This increases complexity and limits the operation frequency. Moreover, in bipolar LTD, electromagnetic interference can be significant.

F. MODULAR MULTILEVEL CONVERTER

Modular Multilevel Converter (MMC) is a widely adopted solution in pulsed power applications due to its inherent advantages of a modular structure, high reliability, fault-tolerant capability, and high efficiency. There are three commonly used submodule [93]. These include symmetrical half-bridge (HB) topology, asymmetrical half-bridge topology, and H-bridge topology, as depicted in Fig. 24.

As shown in Fig. 25, an HB-MMC topology is proposed to generate high-voltage pulses with adjustable rise/fall times in [94]. The topology comprises two arms, with the capacitors charged in parallel. By controlling the discharge sequence, it is possible to generate either unipolar or bipolar pulses. Furthermore, by configuring the switching sequence for each arm, pulses with different parameters can be generated.

MMC can reduce the voltage ratings of switches and provide flexible output waveforms. However, maintaining a balanced voltage across submodule capacitors presents a significant challenge, and the control strategies tend to be complex.

G. HYBRID PULSE GENERATOR

Each individual topology has its strengths and weaknesses. Therefore, combining two or even three topologies can be an appealing approach.

Marx generator is a promising choice for achieving high-voltage levels, but it cannot generate square pluses. By replacing the capacitors with PFNs, the generator can generate

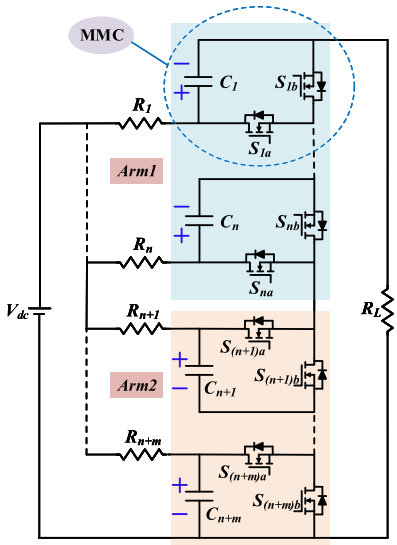

FIGURE 25. Half-bridge MMC-based pulse generator [94].

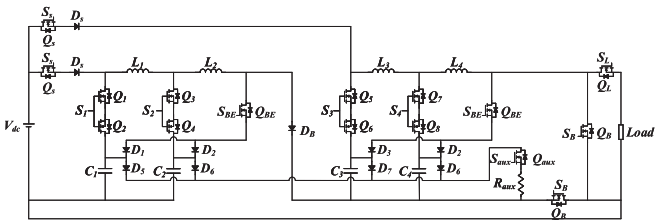

FIGURE 26. Boost converter-PFN-Marx pulse generator [95].

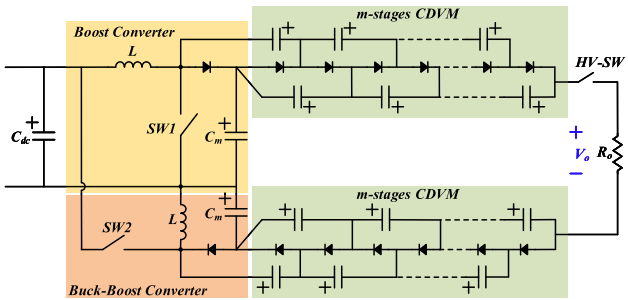

FIGURE 27. Boost and Buck-Boost Converter in conjunction with CDVMs [96].

square pulses with high step-up capability. Fig. 5 illustrates the combination of a boost converter with a PFN. In [95], this system is further improved by integrating it with the Marx circuit, as shown in Fig. 26. The circuit comprises multiple Marx floors and boost-PFN stages to increase the output voltage levels.

DC converters can also be combined with CDVM to achieve higher voltage levels. In [96], the CDVM stages are divided into two groups, one is fed from a boost converter, and the other is fed from a buck-boost converter, as depicted in Fig. 27. Due to the inverted output capability of Buck-Boost converter, which enables series-connection of the boost and

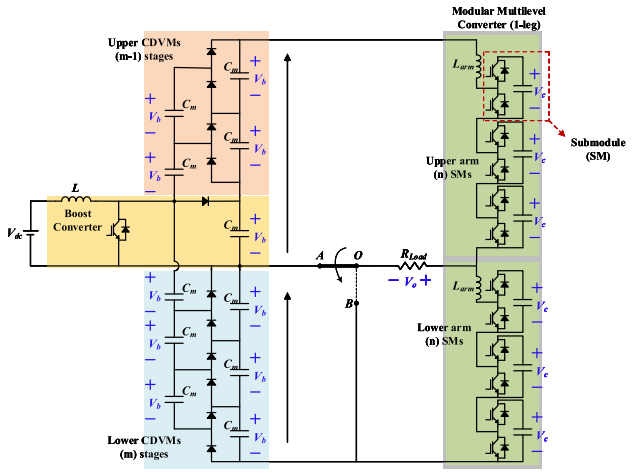

FIGURE 28. Boost Converter in conjunction with CDVMs and MMC [97].

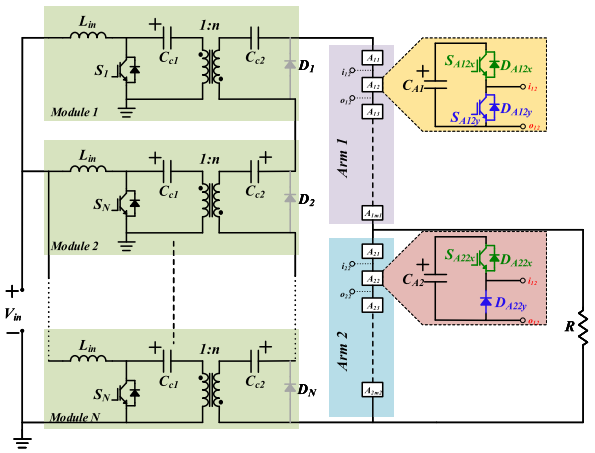

FIGURE 29. Pulse generator based on voltage-boosting modules and MMC-SMs [98].

buck-boost converters with no need for isolated inputs, this structure can reach a higher voltage level.

The aforementioned topology can only generate unipolar pulses. However, in certain applications, bipolar pulses are more suitable. Moreover, these topologies require a high-voltage switch at the output stage to chop the elevated DC voltage into pulses. A similar concept can be applied for bipolar pulse generation, but facilitated by an H-bridge instead of a high-voltage chopping switch. In [97], a central-feeding boost-CDVM is utilized to generate a high-voltage supply, which is then fed to MMC-based pulse generator, as shown in Fig. 28. This generator consists of two identical arms composed of multiple HB SMs. By switching the selector to position (A) or (B), this structure can generate bipolar or unipolar output voltage, respectively.

In [98], a step-up pulse generator fed from a LVDC supply is proposed, utilizing isolated input-parallel/output-series (IPOS) voltage-boosting modules (VBM) and MMC-SMs, as shown in Fig. 29. The capacitors in each VBM are charged simultaneously, allowing for efficient charging. The high

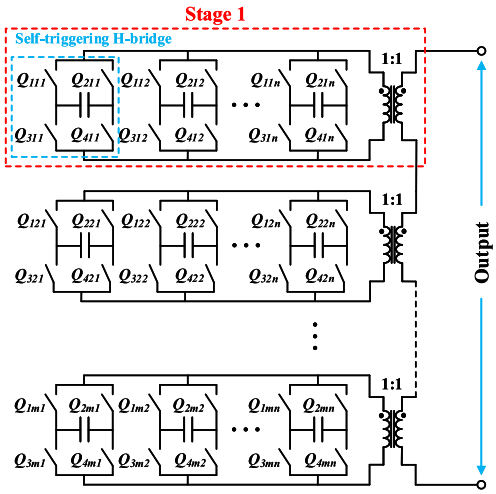

FIGURE 30. LTD topology with self-triggering H-bridge circuit [102].

voltage generated by connecting the outputs of individual VBMs in series is chopped by employing two arms of series-connected MMC-SMs. This approach eliminates the need for high voltage switches and enables the generation of unipolar or bipolar pulses with flexible amplitude, repetition rate, and pulse duration. This structure exhibits good modularity, scalability, and redundancy.

As mentioned earlier, LTD is a commonly used method to increase the pulse amplitude, making it suitable for combining with other topologies such as Marx circuit, SOS circuit, and MMC [99], [100], [101].

A self-triggering H-bridge circuit is introduced into the conventional LTD topology in [102], as shown in Fig. 30. The introduction of a self-triggering H-bridge, not only reduces the control complexity but also allows for higher operation frequency without the need for active demagnetization circuits. The bipolar operation mode ensures that the magnetic core operates in high magnetic permeability region and prevents saturation of the core.

Hybrid generators combine two or more common topologies, incorporating the characteristics of each subcircuit, thereby capable of outputting more flexible and variable pulses. These methods can avoid some limitations of common single topologies, and improve characteristics such as pulse amplitude, pulse polarity, and pulse shape. For example, combining Marx with PFN can output square waves that Marx circuit cannot output, and also improve the pulse amplitude of PFN circuit; combining converter circuit with CDVM can further improve pulse amplitude; combining single pulse generator with MMC or LTD can make the output waveform more flexible and diverse. However, along with these improvements, compared to single pulse generators, the topological complexity of hybrid pulse generators inevitably increases.

So far, we have discussed various pulse generator topologies and summarized their features and limitations in Table 3. Classical generators like Marx generators, PFN, PFL and MPC, tend to be bulky, inefficient and inflexible. On the other

TABLE 3. Summary of Main Groups of Pulse Generator

	Structure	Features	Limitations
Classic Generator	Marx	* High voltage and current * High modularity	* Bulky structure * Limited pulse repetition frequency * Electrode degradation of spark gaps
	PFN	* Limited stored energy * Simple structure	* High voltage source requirement * Pulse width inflexibility * Narrow range of the load
	PFL/BL	* Commonly used for rectangular pulse with 1-100ns pulse width * Simple structure	* High voltage source requirement * Load impedance matching requirement * Pulse width inflexibility
	Tesla Transformer	* Compact design * High efficiency * Simple structure	* Support insulator design * Secondary side stray capacitance
	MPC	* High pulse repetition frequency * High power * High reliability	* Low efficiency * Pulse width inflexibility
Power Electronics Based Generator	Solid-State Marx	* High reliability * High repetition frequency * High modularity	* Driver of switches * Switch synchronization
	SMPS	* Wide flexibility of pulse parameters * Simple structure * High repetition frequency	* HV switch requirement * Complicated control algorithm * Driver of switches
	CDVM	* Pulse width flexibility * AC power supply requirement * High modularity	* HV switch requirement * Limited repetition frequency * Driver of switches
	Circuit Based on SOS	* High energy density * Short pulse application * High pulse repetition frequency	* Complicated design * Pulse width inflexibility * Low output power
	LTD	* High pulse amplitude * Modular structure * Flexible pulse waveforms	* Core saturation and reset * Strong electromagnetic interference * Complex trigger circuit
	MMC	* Wide flexibility of pulse parameters * Fault-tolerant capability * High modularity and scalability	* Complex control algorithm * Limited amplitude resolution * Capacitor voltage balancing * Limited minimum pulse width
	Hybrid	* High flexibility * High scalability	* High complexity

hand, power electronics based generators have advantages of high reliability, flexibility, efficiency, and simplicity in structure. Moreover, certain topologies exhibit high modularity, which makes them suitable for a wide range of industrial applications. By adjusting the control algorithms, some power electronics based generators, such as MMC and LTD, can even generate pulses of multiple shapes with variable parameters [103], [104], [105].

IV. PULSE GENERATORS FOR DIFFERENT APPLICATIONS

In the field of pulsed power technology, there are two main directions of development, each with its own set of challenges and requirements for high-voltage pulse generators. The first direction focuses on increasing the voltage and current levels, aiming to achieve record-high pulsed power. This is primarily utilized in fundamental research fields such as nuclear fusion, X-ray generation, and high-power lasers. One prominent example is the Z machine at Sandia National Laboratories, known for its large-scale pulsed power experiments [106]. In these applications, the key performance indicators are high peak power, while high average power, pulse repetition frequency, and compactness are of lesser important.

The second direction involves the utilization of high-voltage pulses in various applications. These applications span a wide range of fields, including water treatment [107], biomedical applications [108], air treatment [109], food

TABLE 4. List of High-Voltage Pulse Generators with Their Pulse Performance

Reference	Topology	Switch Type	Charging Voltage	Pulse Voltage	Pulse Current	Pulse width	Rise time	Repetition Rate	Pulse waveforms	Load	Application
[90]	LTD	Gas switch	200 kV	100 kV	0.5 MA	132 ns	50 ns	0.097 Hz	Gaussian	Liquid resistor	Z-pinch ICF driver
[24]	Marx	Gas switch	70 kV	550 kV	-	120 ns	32 ns	-	Gaussian	15Ω dummy load	Vacuum diode driver
[46]	PFN + Tesla transformer	Gas switch	900 kV	300 kV	6.9 kA	110 ns	7 ns	10 Hz	Quasi-rectangular	40Ω water load	High-power microwave generators
[30]	PFN + Marx	Gas switch	30 kV	80 kV	-	105 ns	30 ns	-	Quasi-rectangular	30Ω Resistor	High-power microwave generators
[44]	Tesla transformer + PFL	Gas switch	0.5 kV	220 kV	-	13 ns	4 ns	100 Hz	Quasi-rectangular	10Ω dummy load	High-power microwave generators
[23]	Marx + Pulse transformer	Thyristor	1.25 kV	79.6 kV	-	-	141 ns	10 Hz	Gaussian	1kΩ dummy load	High-power intense electron beam accelerator
[50]	MPC + Pulse transformer	Magnetic switch	0.8 kV	13 kV	-	80 ns	100 ns	500 Hz	Gaussian	600Ω resistor	Dielectric barrier discharge
[87]	Circuit based on SOS	DOS + Magnetic switch	0.5 kV	13.3 kV	-	9.7 ns	9.3 ns	12 kHz	Gaussian	50Ω resistor	Low-temperature plasma
[99]	LTD + Marx	AT	1.2 kV	10.9 kV	74 A	10 ns	3.3 ns	-	Gaussian	50Ω resistor	Atmosphere pressure plasma
[91]	LTD	IGBT	5.7 kV	470 kV	5.4 kA	125 ns	-	50 Hz	Quasi-rectangular	100Ω resistor	High-power microwave driver
[78]	CDVM	IGBT	0.4 kV	1.4 kV	-	8 μs	100 ns	110 Hz	Exponential	22Ω resistor	Pulsed power application
[79]	CDVM	IGBT	135 V	2 kV	-	150 μs	2 μs	800 Hz	Quasi-rectangular	10kΩ resistor	Pulsed power application
[97]	CDVM + Boost + MMC	IGBT	50 V	0.8 kV	0.8 A	10 μs	0.1 μs	1 kHz	Quasi-rectangular	1kΩ resistor	Water treatment applications
[62]	Marx	MOSFET	0.8 kV	15.3 kV	20 A	200-1000 ns	45 ns	10 kHz	Exponential	Capacitive branch	Plasma flow control
[13]	Marx	MOSFET	10 kV	30 kV	30 A	500 ns	40 ns	-	Quasi-rectangular	1kΩ resistor	Plasma flow control
[103]	LTD	MOSFET	1 kV	29 kV	240 A	50-170 ns	30-40 ns	100 Hz	Gaussian / Quasi-rectangular	120Ω resistor	Gas discharge
[71]	Forward	MOSFET	0.5 kV	6.5 kV	0.3 A	5 μs	1 μs	10 kHz	Quasi-rectangular	Plasma load	Plasma immersion ion implantation
[94]	MMC	MOSFET	0.5 kV	2 kV	-	100-500 ns	15-65 ns	1 kHz	Quasi-rectangular	200Ω resistor	Plasma discharge
[102]	MMC + LTD	MOSFET	0.5 kV	2.5 kV	2.5 A	60-260 ns	11 ns	10 kHz	Quasi-rectangular	Capacitive branch	Tumor treatment
[34]	BL + TLT	MOSFET	1.5 kV	10 kV	25 A	30 ns	13.7 ns	100 kHz	Gaussian	400Ω resistor	Tumor treatment
[95]	Marx + PFN + Boost	MOSFET	4 V	23.6 V	-	8 μs	1.412 μs	166 Hz	Exponential	1Ω resistor	Dielectric barrier discharge
BEHLKE GHTS 60A [114]	-	MOSFET	-	6 kV	30 A	100 ns - ∞	12 ns	20 kHz	Rectangular	Any load type	Laboratory use
BEHLKE FSWP 91-01 [115]	-	MOSFET	-	9 kV	15 A	50 ns - ∞	10 ns	50 kHz	Rectangular	Any load type	-
PULSE RPG-C-10-100-5P [116]	-	Solid state semiconductors	-	10 kV	100 A	20 ns - ∞	5 ns	20 kHz	Rectangular	Any load type	Plasma science research
PULSE APG-C-40-100 [117]	-	Solid state semiconductors	-	40 kV	100 A	40 ns - ∞	10-150 ns	1 kHz	Rectangular	Capacitive load	Plasma science research
NORTH STAR SP-55 [118]	Pulse transformer	Solid state switch	-	55 kV	-	300 ns	<130 ns	-	Gaussian	Spark gaps	Spark gap trigger system
SYDOR 10 kV Pulser [119]	-	-	110 VAC, 60 Hz	10 kV	-	10-110 ns	<10 ns	5 Hz	Rectangular	50Ω	Pockels cell driver
BNC PVX-4130 [120]	Totem pole	-	90-240 VAC, 50/60 Hz	±6 kV	-	150 ns - ∞	<60 ns	10 kHz	Rectangular	Capacitive load	Pockels cell driver
ABSOLUTE EMC PG 20-4000 [121]	-	-	230 VAC, 50/60 Hz	1-20 kV	25-500 A	-	10 μs	60 Hz	Rectangular	Capacitive load	EMC test
HPPI TLP-12010C [121]	-	-	100-240 VAC, 47-63 Hz	±6 kV	120 A	100 ns	0.3-50 ns	5 Hz	Rectangular	-	ESD measurement

processing [110], and others [111], [112], [113]. In these cases, the pulses are characterized by high repetition frequency, compactness, and reliability. These applications often require high-voltage pulse generators that can operate at high frequency while maintaining a small footprint and ensuring reliable performance. The precise control over the output pulses may also be needed to meet specific requirements.

Both directions rely on the use of high-voltage pulse generators, but their specific requirements and priorities may vary. It is important to consider the unique challenges and characteristics of each application when designing and selecting pulse generator topologies.

Furthermore, high-voltage pulse generators for different applications are analyzed and classified. Several generators and commercialized products are listed in Table 4, with the following parameters reported: topology, switch type, charging voltage, pulse voltage amplitude, pulse current amplitude, pulse width, rise time, repetition rate, pulse waveforms, and load type, as well as the potential applications for each generator. For commercialized products, the rise time represents fastest rising edge, but it will also be affected by the actual load characteristics. The applications enumerated in the table are not exclusive, any applications exhibiting similar load characteristics can be feasibly extrapolated.

All topologies demonstrate the capability to produce high-voltage pulses. However, classical topologies employing gas switches excel in producing pulses with extremely high amplitude, exceeding 100 kV. The performance and characteristics of switches are instrumental in determining the attributes of the pulses. Gas switches, although capable of tolerating high voltages and currents, encounter challenges such as electrode erosion, limited control over pulse duration, and a comparatively shorter lifetime. They are more suitable for ultra-high-voltage scenarios, such as the triggering of megavolt switches.

Conversely, semiconductor switches offer enhanced flexibility in pulse shaping and the ability to operate at high repetition rates. Despite these advantages, they are constrained by limitations when subjected to high voltages and currents. Employing series-connected switches can mitigate high voltage constraints, but this approach introduces its own set of complications. Specifically, the added stray inductance that can degrade the overall performance.

V. CHALLENGES AND TRENDS

A. DEVICE DEVELOPMENT

All the mentioned topologies demonstrate the ability to generate high-voltage pulses. The classical Marx circuit and transmission line topologies, which use spark gap switches, can generate pulses with very high amplitudes, often exceeding 100 kV. However, these designs come with a level of complexity. With the recent development of solid-state topologies, there is a growing availability of off-the-shelf semiconductors that meet the high-voltage requirements. The research priority for future development is to achieve high power density. The utilization of semiconductor switches makes high-voltage generators smaller and lighter.

In some solid-state topologies, series-connected semiconductors are used instead of high-voltage switches. The emergence of wide bandgap (WBG) semiconductor switches, such as SiC and GaN switches, has further improved performance. These WBG devices offer advantages like high bandgap, high saturation drift velocity, high breakdown electric field, and low on-state resistance. Replacing traditional Si switches by WBG switches allows for higher power and repetition rate [122], [123], [124]. This, in turn, enables a significant

reduction in the size of magnetic components due to the higher repetition rate.

However, there are some challenges to address. In contrast to Si devices, the current and voltage ratings of commercial WBG devices are relatively low. To date, high-voltage high-current commercial products are still unavailable [125]. Specifically, the voltage ratings of SiC and GaN devices are limited to 3.3 kV and 900 V, respectively, while those of Si devices can exceed 4.7 kV. Additionally, WBG devices tend to be more expensive and raise concerns about reliability. For instance, studies indicate that in high-current applications, the cost of SiC MOSFETs is approximately eight times that of Si IGBTs [126].

Furthermore, the switching characteristics of these devices are strongly dependent on the gate drive circuit. The gate drive circuit requires careful consideration of various external switching factors, including parasitic elements, circuit components, and PCB layout [127]. Traditional commercial gate drivers, often using push-pull or totem-pole driving topologies, are not suitable for high-current switching with rise times on the order of 10-20 ns [128]. Moreover, when multiple switches are connected in series or parallel, the switching synchronization is also important. Therefore, when using wide bandgap switches, special attention must also be paid to the gate driving circuitry.

B. THERMAL MANAGEMENT

As we mentioned before, with the increasing application of semiconductor switches, reliability becomes the crucial issue. Temperature is the main cause of malfunction and eventual failure in electronics, and therefore, reliability is strongly dependent on it: the higher the temperature, the worse the reliability and durability [129]. Therefore, thermal management is a key design aspect of pulse generators as it determines their reliability as well as pulse performance and power density.

Firstly, thermal management requires accurate loss calculation and temperature measurement technology [130]. In [131], the power losses and current distribution in soft- and hard-switched IGBTs under resonant load are studied. Among the existing techniques for noninvasive thermal measurements, infrared thermography (IR) combined with a lock-in detection strategy has been widely used [132], [133]. In [134], accurate transient calorimetric measurement of soft-switching losses of 10-kV SiC MOSFETs and diodes is presented, which provides a solid basis for accurate modeling of systems.

In addition to establishing more accurate loss models and thermal models, cooling technologies are also a research hotspot [135], [136], [137]. In [138], different cooling technologies are introduced, and the conventional single-phase water/glycol liquid cooling and innovative two-phase cooling technology for thermal management are compared. It shows that two-phase cooling, using the same cold plate as in single-phase cooling, can substantially improve performance and reliability. In [139], the two-phase immersion cooling technique is used to improve the performance of a high-voltage pulse generator based on avalanche transistors. With this cooling method, the surface temperature of the transistor can be effectively controlled below 62°C when it is working at a frequency of 200 kHz.

Active thermal control is another strategy to reduce the junction temperature of the most stressed devices, which can minimize design margins [140], [141], [142]. A comprehensive review of active thermal control is presented in [143], where the implementation of active thermal control is investigated at the device and converter levels. Furthermore, the challenges in different applications of active thermal control are discussed.

C. MINIATURIZATION

In many applications, such as electromagnetic gun, electroporation, and high power microwaves, an appropriate size and weight of pulsed power systems are prerequisites for their widespread use, which require high power density and miniaturization. Therefore, the development of miniaturized, highly reliable, and low-cost systems is essential for long-term growth. It is also a necessary step towards the industrialization and practical application of pulsed power technologies. The miniaturization of high-voltage pulse generators is one of the research directions in the future [144]. In addition, miniaturization often accompanies a compact structure, which reduces the connection inductance between the capacitor and the switch, thereby improving the output pulse performance. Many studies have demonstrated the efforts of researchers in the miniaturization of pulsed power systems [145], [146].

D. THEORETICAL ANALYSIS AND MODELING

For various applications, the load characteristics exhibit significant diversity. HVPGs rely on the performance and characteristics of semiconductors, which may differ from the load characteristics. Therefore, it is necessary to analyze the load characteristics of various applications when using wide bandgap semiconductors. This is particularly important as the load characteristics can vary significantly under high-frequency operation.

Furthermore, conducting research on actual processing and experiments is crucial. The practical load characteristics provide guidance to the optimization of pulse generators, leading to higher efficiency and improved pulse performance. It is a cyclical process, where the most suitable circuit parameters and pulse performance for a specific application are determined through experiment and analysis.

VI. CONCLUSION

This paper provides a comprehensive review of various HVPG topologies for different applications. The topologies are broadly classified into classical HVPGs, and power electronics based HVPGs. Each method is further categorized based on topology characteristics and operation modes, with a discussion of their features and limitations.

The paper begins by outlining the common structure of each topology and any modifications that have been made. It then

introduces typical applications of HVPGs. Finally, the future trends in HVPG design are analyzed based on recent topology evolvements, including reducing volume and weight through the use of WBG devices, improving reliability through proper thermal management, and theoretical analysis and modeling for more accurate design.

The advancements of power semiconductors and converters promote the developments of HVPG topologies, which also benefit the applications utilizing HVPGs. Designing and developing high-voltage pulse generators that are suitable for specific applications is a challenging task due to varying requirements such as isolation, controllability, voltage amplitude, and pulse width. Choosing the best solution involves a tradeoff among cost, size, efficiency, and pulse characteristics. The aim of this paper is to provide a clear overview of high-voltage pulse generators and inspire the development of new topologies to meet specific requirements.

REFERENCES

[1] J. T. Camp et al., "Cell death induced by subnanosecond pulsed electric fields at elevated temperatures," *IEEE Trans. Plasma Sci.*, vol. 40, no. 10, pp. 2334–2347, Oct. 2012.

[2] Z. Fang, Z. Ding, T. Shao, and C. Zhang, "Hydrophobic surface modification of epoxy resin using an atmospheric pressure plasma jet array," *IEEE Trans. Dielectrics Elect. Insul.*, vol. 23, no. 4, pp. 2288–2293, Aug. 2016.

[3] M. X. Gao et al., "Traveling-wave Marx circuit for generating repetitive sub-nanosecond pulses," *IEEE Trans. Electromagn. Compat.*, vol. 61, no. 4, pp. 1271–1279, Aug. 2019.

[4] J. Yan, S. Parker, and S. Bland, "An investigation into high-voltage spiral generators utilizing thyristor input switches," *IEEE Trans. Power Electron.*, vol. 36, no. 9, pp. 10005–10019, Sep. 2021.

[5] S. Shen, J. Yan, G. Sun, and W. Ding, "Improved auxiliary triggering topology for high-power nanosecond pulse generators based on avalanche transistors," *IEEE Trans. Power Electron.*, vol. 36, no. 12, pp. 13634–13644, Dec. 2021.

[6] Y. Gu, C. Zhang, W. Bian, S. Wu, and Z. Xu, "A novel modular pulse generator with high voltage gain and reduced number of capacitors," *IEEE Trans. Plasma Sci.*, vol. 50, no. 2, pp. 394–400, Feb. 2022.

[7] H. S. Kim, C. H. Yu, S. R. Jang, and G. H. Kim, "Solid-state pulsed power modulator with fast rising/falling time and high repetition rate for pockels cell drivers," *IEEE Trans. Ind. Electron.*, vol. 66, no. 6, pp. 4334–4343, Jun. 2019.

[8] X. Cheng, S. Chen, Y. Lv, H. Chen, and B. M. Novac, "An improved high voltage pulse generator with few nanoseconds based on the synergy of DOS and LTD topologies for supra electroporation," *IEEE Trans. Ind. Electron.*, vol. 70, no. 8, pp. 7855–7866, Aug. 2023.

[9] S. N. Rukin, "Pulsed power technology based on semiconductor opening switches: A review," *Rev. Sci. Instrum.*, vol. 91, no. 1, Jan. 2020, Art. no. 011501.

[10] Z. Liu, A. J. M. Pemen, R. T. W. J. Van Hoppe, G. J. J. Winands, E. J. M. Van Heesch, and K. Yan, "An efficient, repetitive nanosecond pulsed power generator with ten synchronized spark gap switches," *IEEE Trans. Dielectrics Elect. Insul.*, vol. 16, no. 4, pp. 918–925, Aug. 2009.

[11] M. A. Elgenedy, A. M. Massoud, S. Ahmed, and B. W. Williams, "A high-gain, high-voltage pulse generator using sequentially charged modular multilevel converter submodules, for water disinfection applications," *IEEE J. Emerg. Sel. Topics Power Electron.*, vol. 6, no. 3, pp. 1394–1406, Sep. 2018.

[12] L. Cheng et al., "High-voltage repetitive nanosecond pulse generator utilizing power synthesis of modified avalanche transistorized Marx circuits," *IEEE Trans. Instrum. Meas.*, vol. 71, 2022, Art. no. 2002816.

[13] L. Pang, T. Long, K. He, Y. Huang, and Q. Zhang, "A compact series-connected SiC MOSFETs module and its application in high voltage nanosecond pulse generator," *IEEE Trans. Ind. Electron.*, vol. 66, no. 12, pp. 9238–9247, Dec. 2019.

[14] G. Duan, S. N. Vainshtein, and J. T. Kostamovaara, "Modified high-power nanosecond Marx generator prevents destructive current filamentation," *IEEE Trans. Power Electron.*, vol. 32, no. 10, pp. 7845–7850, Oct. 2017.

[15] H. Niu and R. D. Lorenz, "Evaluating different implementations of online junction temperature sensing for switching power semiconductors," *IEEE Trans. Ind. Appl.*, vol. 53, no. 1, pp. 391–401, Jan. 2017.

[16] H. Niu and R. D. Lorenz, "Real-time junction temperature sensing for silicon carbide MOSFET with different gate drive topologies and different operating conditions," *IEEE Trans. Power Electron.*, vol. 33, no. 4, pp. 3424–3440, Apr. 2018.

[17] A. Sheikholeslami and J. Adabi, "High-voltage pulsed power supply to generate wide pulses combined with narrow pulses," *IEEE Trans. Plasma Sci.*, vol. 42, no. 7, pp. 1894–1901, Jul. 2014.

[18] M. Hochberg et al., "A fast modular semiconductor-based Marx generator for driving dynamic loads," *IEEE Trans. Plasma Sci.*, vol. 47, no. 1, pp. 627–634, Jan. 2019.

[19] H. Sarnago, O. Lucia, A. Naval, J. M. Burdio, Q. Castellvi, and A. Ivorra, "A versatile multilevel converter platform for cancer treatment using irreversible electroporation," *IEEE J. Emerg. Sel. Topics Power Electron.*, vol. 4, no. 1, pp. 236–242, Mar. 2016.

[20] M. N. Uddin, H. Allahyari, Y. H. Tabriz, and H. Bahrami, "A solid-state bipolar pulse power generator for dielectric barrier discharge applications," *IEEE Trans. Ind. Appl.*, vol. 58, no. 6, pp. 7942–7951, Nov./Dec. 2022.

[21] Z. Zhong, J. Rao, H. Liu, and L. M. Redondo, "Review on solid-state-based Marx generators," *IEEE Trans. Plasma Sci.*, vol. 49, no. 11, pp. 3625–3643, Nov. 2021.

[22] X. Guo, D. Zheng, and F. Blaabjerg, "Power electronic pulse generators for water treatment application: A review," *IEEE Trans. Power Electron.*, vol. 35, no. 10, pp. 10285–10305, Oct. 2020.

[23] J. Y. Geng, J. H. Yang, X. B. Cheng, R. Chen, and T. Shu, "A compact, low jitter, high voltage trigger generator based on fractional-turn ratio saturable pulse transformer and its application," *Rev. Sci. Instrum.*, vol. 93, no. 8, Aug. 2022, Art. no. 084709.

[24] H. Liu, P. Jiang, J. Yuan, L. Wang, X. Ma, and W. Xie, "A novel compact low impedance Marx generator with quasi-rectangular pulse output," *Rev. Sci. Instrum.*, vol. 89, no. 4, Apr. 2018, Art. no. 044703.

[25] G. Yanqing et al., "A compact repetitive Marx generator with fast rise-time," *High Power Laser Part. Beams*, vol. 25, no. S0, pp. 164–168, May 2013.

[26] F. Song et al., "Recent advances in compact repetitive high-power Marx generators," *Laser Part. Beams*, vol. 37, no. 1, pp. 110–121, Mar. 2019.

[27] J. Clementson, K. Rahbarnia, O. Grulke, and T. Klinger, "Design of A, B, and C pulse forming networks using the VINPFN application," *IEEE Trans. Power Electron.*, vol. 29, no. 11, pp. 5673–5679, Nov. 2014.

[28] F. Li, F. Song, M. Zhu, X. Jin, Y. Gan, and H. Gong, "A compact high-voltage pulse forming module with hundreds of nanoseconds quasi-squared output pulse," *Rev. Sci. Instrum.*, vol. 89, no. 10, Oct. 2018, Art. no. 104706.

[29] H. Zhang, J. Yang, J. Lin, and X. Yang, "A compact bipolar pulse-forming network-Marx generator based on pulse transformers," *Rev. Sci. Instrum.*, vol. 84, no. 11, Nov. 2013, Art. no. 114705.

[30] H. Zhang, Z. Li, Z. Zhang, and T. Shu, "Investigation on the generation of high voltage quasi-square pulses with a specific two-node PFN-Marx circuit," *Rev. Sci. Instrum.*, vol. 91, no. 2, Feb. 2020, Art. no. 024702.

[31] S. M. Hosseini and H. R. Ghaforinam, "Improving the pulse generator BOOST PFN to increase the amplitude and decrease the pulse duration of the voltage," *IEEE Trans. Dielectrics Elect. Insul.*, vol. 23, no. 3, pp. 1699–1704, Jun. 2016.

[32] L. Wang and J. Liu, "Solid-state nanosecond pulse generator using photoconductive semiconductor switch and helical pulse forming line," *IEEE Trans. Plasma Sci.*, vol. 45, no. 12, pp. 3240–3245, Dec. 2017.

[33] Y. Mi, C. Bian, J. Wan, J. Xu, C. Yao, and C. Li, "A modular solid-state nanosecond pulsed generator based on Blumlein-line and transmission line transformer with microstrip line," *IEEE Trans. Dielectrics Elect. Insul.*, vol. 24, no. 4, pp. 2196–2202, Apr. 2017.

[34] Y. Mi, C. Bian, P. Li, C. Yao, and C. Li, "A modular generator of nanosecond pulses with adjustable polarity and high repetition rate," *IEEE Trans. Power Electron.*, vol. 33, no. 12, pp. 10654–10662, Dec. 2018.

[35] Y. Mi, J. Wan, C. Bian, Y. Zhang, C. Yao, and C. Li, "A multiparameter adjustable, portable high-voltage nanosecond pulse generator based on stacked Blumlein multilayered PCB strip transmission line," *IEEE Trans. Plasma Sci.*, vol. 44, no. 10, pp. 2022–2029, Oct. 2016.

[36] Y. Zhao et al., "Replacement of Marx generator by Tesla transformer for pulsed power system reliability improvement," *IEEE Trans. Plasma Sci.*, vol. 47, no. 1, pp. 574–580, Jan. 2019.

[37] L. Li et al., "Study on double resonant performance of air-core spiral Tesla transformer applied in repetitive pulsed operation," *IEEE Trans. Dielectrics Elect. Insul.*, vol. 22, no. 4, pp. 1916–1923, Aug. 2015.

[38] G. A. Mesyats et al., "Repetitively pulsed high-current accelerators with transformer charging of forming lines," *Laser Part. Beams*, vol. 21, no. 2, pp. 197–209, Apr. 2003.

[39] G. Mesyats, S. Korovin, V. Rostov, V. Shpak, and M. Yalandin, "The RADAN series of compact pulsed power generators and their applications," *Proc. IEEE*, vol. 92, no. 7, pp. 1166–1179, Jul. 2004.

[40] L. Zhao et al., "A compact multi-wire-layered secondary winding for Tesla transformer," *Rev. Sci. Instrum.*, vol. 88, no. 5, May 2017, Art. no. 055112.

[41] L. Zhao et al., "Prolonging the lifetime of a compact multi-wire-layered secondary winding in the Tesla transformer," *Rev. Sci. Instrum.*, vol. 93, no. 4, Apr. 2022, Art. no. 044703.

[42] L. Zhao, R. Li, Y. Zhang, X. D. Xu, W. Shang, and X. D. Qiu, "Design and test of a copper-titanium-composite primary winding for Tesla transformer," *IEEE Trans. Plasma Sci.*, vol. 50, no. 9, pp. 3155–3159, Sep. 2022.

[43] M. Istenic, B. M. Novac, J. Luo, R. Kumar, and I. R. Smith, "A 1-mV magnetically insulated Tesla transformer," *IEEE Trans. Plasma Sci.*, vol. 36, no. 5, pp. 2644–2650, Oct. 2008.

[44] S. Liu et al., "Low-impedance high-power pulsed generator based on forming line with built-in Tesla transformer," *Rev. Sci. Instrum.*, vol. 92, no. 8, Aug. 2021, Art. no. 084705.

[45] J.-C. Su et al., "A coaxial-output rolled strip pulse forming line based on multi-layer films," *Laser Part. Beams*, vol. 36, no. 1, pp. 69–75, Mar. 2018.

[46] J. Su et al., "A long-pulse generator based on Tesla transformer and pulse-forming network," *IEEE Trans. Plasma Sci.*, vol. 37, no. 10, pp. 1954–1958, Oct. 2009.

[47] J. Su et al., "An 8-GW long-pulse generator based on Tesla transformer and pulse forming network," *Rev. Sci. Instrum.*, vol. 85, no. 6, Jun. 2014, Art. no. 063303.

[48] M. Wang, B. M. Novac, L. Pécastaing, and I. R. Smith, "Bipolar modulation of the output of a 10-GW pulsed power generator," *IEEE Trans. Plasma Sci.*, vol. 44, no. 10, pp. 1971–1977, Oct. 2016.

[49] D. Zhang, Y. Zhou, J. Wang, and P. Yan, "A compact, high repetition-rate, nanosecond pulse generator based on magnetic pulse compression system," *IEEE Trans. Dielectrics Elect. Insul.*, vol. 18, no. 4, pp. 1151–1157, Aug. 2011.

[50] Y. Mi, J. Wan, C. Bian, Y. Zhang, C. Yao, and C. Li, "A high-repetition-rate bipolar nanosecond pulse generator for dielectric barrier discharge based on a magnetic pulse compression system," *IEEE Trans. Plasma Sci.*, vol. 46, no. 7, pp. 2582–2590, Jul. 2018.

[51] M. D. Evans, V. J. Baillard, P. D. Maqueo, J. M. Bergthorson, and S. Coulombe, "Compact nanosecond magnetic pulse compression generator for high-pressure diffuse plasma generation," *IEEE Trans. Plasma Sci.*, vol. 45, no. 8, pp. 2358–2365, Aug. 2017.

[52] D. K. Singh, B. Dikshit, N. O. Kawade, J. Mukherjee, and V. S. Rawat, "Exploration of jitter in solid-state switch-based pulse power supply of copper vapor laser," *J. Russian Laser Res.*, vol. 41, no. 6, pp. 628–637, Nov. 2020.

[53] Y. Liu, S. Liu, Y. Han, Y. Ge, Q. Zhang, and F. Lin, "Optimization design of a repetitive nanosecond pulse generator based on saturable pulse transformer and magnetic switch," *IEEE Trans. Plasma Sci.*, vol. 43, no. 9, pp. 3277–3285, Sep. 2015.

[54] Y. Zhang and J. Liu, "Physical suppression effects of the reversed magnetic coupling on the saturation inductance of saturable pulse transformer," *Appl. Phys. Lett.*, vol. 102, no. 25, Jun. 2013, Art. no. 253502.

[55] S. H. Kim, J. B. Park, S. D. Choi, Y. H. Kim, and M. Ehsani, "Optimal control method of magnetic switch used in high-voltage power supply," *IEEE Trans. Power Electron.*, vol. 28, no. 3, pp. 1065–1071, Mar. 2013.

[56] S. H. Kim and M. Ehsani, "Control and analysis of magnetic switch reset current in pulsed power systems," *IEEE Trans. Power Electron.*, vol. 29, no. 2, pp. 529–533, Feb. 2014.

[57] J. Rao, K. Liu, and J. Qiu, "All solid-state nanosecond pulsed generators based on Marx and magnetic switches," *IEEE Trans. Dielectrics Elect. Insul.*, vol. 20, no. 4, pp. 1123–1128, Aug. 2013.

[58] V. Gamaleev, N. Shimizu, and M. Hori, "Nanosecond-scale impulse generator for biomedical applications of atmospheric-pressure plasma technology," *Rev. Sci. Instrum.*, vol. 93, no. 5, May 2022, Art. no. 053503.

[59] X. Cheng, B. Huang, C. Zhang, F. Kong, Z. Luo, and T. Shao, "A nanosecond pulsed generator with fast-solid-state switch for synchronous discharge in plasma synthetic jet actuators," *IEEE Trans. Plasma Sci.*, vol. 47, no. 5, pp. 1901–1908, May 2019.

[60] S. M. Park, S. H. Song, H. B. Jo, W. C. Jeong, S. R. Jang, and H. J. Ryoo, "Solid-state pulsed power modulator for 9.3 GHz 1.7 mW X-band magnetron," *IEEE Trans. Ind. Electron.*, vol. 68, no. 2, pp. 1148–1154, Feb. 2021.

[61] J. Ma, L. Yu, W. Sun, S. Dong, L. Gao, and C. Yao, "Investigation and evaluation of solid-state Marx pulse generator based on 3-D busbar," *IEEE Trans. Plasma Sci.*, vol. 49, no. 5, pp. 1597–1604, May 2021.

[62] W. Zeng et al., "Self-triggering high-frequency nanosecond pulse generator," *IEEE Trans. Power Electron.*, vol. 35, no. 8, pp. 8002–8012, Aug. 2020.

[63] X. Lan, M. Long, X. Zi-Jie, X. Qin, Z. De-Qing, and Y. Zi-Kang, "A novel generator for high-voltage bipolar square pulses with applications in sterilization of microorganism," *IEEE Trans. Dielectrics Elect. Insul.*, vol. 22, no. 4, pp. 1887–1895, Aug. 2015.

[64] C. Yao, S. Dong, Y. Zhao, Y. Mi, and C. Li, "A novel configuration of modular bipolar pulse generator topology based on Marx generator with double power charging," *IEEE Trans. Plasma Sci.*, vol. 44, no. 10, pp. 1872–1878, Oct. 2016.

[65] Y. Liu, R. Fan, X. Zhang, Z. Tu, and J. Zhang, "Bipolar high voltage pulse generator without H-bridge based on cascade of positive and negative Marx generators," *IEEE Trans. Dielectrics Elect. Insul.*, vol. 26, no. 2, pp. 476–483, Apr. 2019.

[66] Y. He et al., "A polarity-adjustable nanosecond pulse generator suitable for high impedance load," *IEEE Trans. Plasma Sci.*, vol. 48, no. 10, pp. 3409–3417, Oct. 2020.

[67] J. Rao, W. Zhang, S. Jiang, and Z. Li, "Nanosecond pulse generator based on cascaded avalanche transistors and Marx circuits," *IEEE Trans. Dielectrics Elect. Insul.*, vol. 26, no. 2, pp. 374–380, Apr. 2019.

[68] J. Yan, S. Shen, and W. Ding, "High-power nanosecond pulse generators with improved reliability by adopting auxiliary triggering topology," *IEEE Trans. Power Electron.*, vol. 35, no. 2, pp. 1353–1364, Feb. 2020.

[69] L. Cheng et al., "A novel avalanche transistor-based nanosecond pulse generator with a wide working range and high reliability," *IEEE Trans. Instrum. Meas.*, vol. 70, 2021, Art. no. 9002714.

[70] R. Khosravi and M. Rezanejad, "A new pulse generator with high voltage gain and reduced components," *IEEE Trans. Ind. Electron.*, vol. 66, no. 4, pp. 2795–2802, Apr. 2019.

[71] L. M. Redondo and J. F. Silva, "Flyback versus forward switching power supply topologies for unipolar pulsed-power applications," *IEEE Trans. Plasma Sci.*, vol. 37, no. 1, pp. 171–178, Jan. 2009.

[72] A. Elserougi, S. Ahmed, and A. Massoud, "A boost converter-based ringing circuit with high-voltage gain for unipolar pulse generation," *IEEE Trans. Dielectrics Elect. Insul.*, vol. 23, no. 4, pp. 2088–2094, Aug. 2016.

[73] A. Elserougi, A. Massoud, and S. Ahmed, "Multimodule boost-converter-based pulse generators: Design and operation," *IEEE Trans. Plasma Sci.*, vol. 48, no. 1, pp. 219–227, Jan. 2020.

[74] S. Zabihi, F. Zare, G. Ledwich, A. Ghosh, and H. Akiyama, "A new pulsed power supply topology based on positive buck-boost converters concept," *IEEE Trans. Dielectrics Elect. Insul.*, vol. 17, no. 6, pp. 1901–1911, Dec. 2010.

[75] A. Elserougi, A. M. Massoud, and S. Ahmed, "A boost-inverter-based bipolar high-voltage pulse generator," *IEEE Trans. Power Electron.*, vol. 32, no. 4, pp. 2846–2855, Apr. 2017.

[76] L. M. Redondo, "A DC voltage-multiplier circuit working as a high-voltage pulse generator," *IEEE Trans. Plasma Sci.*, vol. 38, no. 10, pp. 2725–2729, Oct. 2010.

[77] M. Rezanejad, J. Adabi, A. Sheikholeslami, and A. Nami, "High-voltage pulse generators based on capacitor-diode voltage multiplier," in *Proc. IEEE 15th Int. Power Electron. Motion Control Conf.*, 2012, pp. LS3c.4-1–LS3c.4-6.

[78] M. R. Delshad, M. Rezanejad, and A. Sheikholeslami, "A new modular bipolar high-voltage pulse generator," *IEEE Trans. Ind. Electron.*, vol. 64, no. 2, pp. 1195–1203, Feb. 2017.

[79] M. Rezanejad, A. Sheikholeslami, and J. Adabi, "Modular switched capacitor voltage multiplier topology for pulsed power supply," *IEEE Trans. Dielectrics Elect. Insul.*, vol. 21, no. 2, pp. 635–643, Apr. 2014.

[80] M. Samizadeh Nikoo and S. M. A. Hashemi, "High-power nanosecond pulse generator with high-voltage SRD and GDT switch," *IEEE Trans. Plasma Sci.*, vol. 43, no. 9, pp. 3268–3276, Sep. 2015.

[81] A. S. Kesar, "A compact, 10-kV, 2-ns risetime pulsed-power circuit based on off-the-shelf components," *IEEE Trans. Plasma Sci.*, vol. 46, no. 3, pp. 594–597, Mar. 2018.

[82] M. Samizadeh Nikoo, S. M. A. Hashemi, and F. Farzaneh, "A two-stage DSRD-Based high-power nanosecond pulse generator," *IEEE Trans. Plasma Sci.*, vol. 46, no. 2, pp. 427–433, Feb. 2018.

[83] A. I. Gusev, M. S. Pedos, A. V. Ponomarev, S. N. Rukin, S. P. Timoshenkov, and S. N. Tsyranov, "A 30 GW subnanosecond solid-state pulsed power system based on generator with semiconductor opening switch and gyromagnetic nonlinear transmission lines," *Rev. Sci. Instrum.*, vol. 89, no. 9, Sep. 2018, Art. no. 094703.

[84] S. Korotkov, Y. Aristov, and A. Zhmodikov, "Comparative studies of high-voltage diode-dynistor generators of high-power nanosecond pulses," *IEEE Trans. Plasma Sci.*, vol. 50, no. 4, pp. 954–958, Apr. 2022.

[85] I. Grekhov, V. Efanov, A. Kardo-Sysoev, and S. Shenderey, "Power drift step recovery diodes (DSRD)," *Solid-State Electron.*, vol. 28, no. 6, pp. 597–599, 1985.

[86] I. Grekhov and G. Mesyats, "Physical basis for high-power semiconductor nanosecond opening switches," *IEEE Trans. Plasma Sci.*, vol. 28, no. 5, pp. 1540–1544, Oct. 2000.

[87] Z. Deng, Z. Ding, Q. Yuan, W. Ding, L. Ren, and Y. Wang, "High voltage nanosecond pulse generator based on diode opening switch and magnetic switch," *Rev. Sci. Instrum.*, vol. 92, no. 6, Jun. 2021, Art. no. 064713.

[88] J. Yang, Y. Xie, Y. Lai, Y. Qiu, and H. Wang, "Study on all-solid high repetition-rate pulse generator based on DSRD," *IEEE Lett. Electromagn. Compat. Pract. Appl.*, vol. 2, no. 4, pp. 142–146, Feb. 2022.

[89] M. R. Kazemi, T. Sugai, A. Tokuchi, and W. Jiang, "Waveform control of pulsed-power generator based on solid-state LTD," *IEEE Trans. Plasma Sci.*, vol. 45, no. 2, pp. 247–251, Feb. 2017.

[90] M. G. Mazarakis et al., "High current, 0.5-ma, fast, 100-ns, linear transformer driver experiments," *Phys. Rev. ST Accel. Beams*, vol. 12, no. 5, May 2009, Art. no. 050401.

[91] L.-M. Wang, Z.-Q. Zhang, Q.-X. Liu, and T.-X. Zhang, "Development of a 500-kV all solid-state linear transformer driver," *IEEE Trans. Plasma Sci.*, vol. 49, no. 6, pp. 1915–1919, Jun. 2021.

[92] Z. Deng, Q. Yuan, W. Ding, Y. Wang, L. Ren, and Z. Wan, "Self-triggering topology for high-power nanosecond pulse generators based on avalanche transistors Marx bank circuits and linear transformer driver," *Rev. Sci. Instrum.*, vol. 93, no. 5, May 2022, Art. no. 054702.

[93] M. A. Perez, S. Bernet, J. Rodriguez, S. Kouro, and R. Lizana, "Circuit topologies, modeling, control schemes, and applications of modular multilevel converters," *IEEE Trans. Power Electron.*, vol. 30, no. 1, pp. 4–17, Jan. 2015.

[94] Y. Mi, H. Wan, C. Bian, W. Peng, and L. Gui, "An MMC-based modular unipolar/bipolar high-voltage nanosecond pulse generator with adjustable rise/fall time," *IEEE Trans. Dielectrics Elect. Insul.*, vol. 26, no. 2, pp. 515–522, Apr. 2019.

[95] S. M. H. Hosseini, H. R. Ghafourinam, and M. H. Oshtaghi, "Modeling and construction of Marx impulse generator based on boost converter pulse-forming network," *IEEE Trans. Plasma Sci.*, vol. 46, no. 10, pp. 3257–3264, Oct. 2018.

[96] A. Elserougi, A. M. Massoud, A. M. Ibrahim, and S. Ahmed, "A high voltage pulse-generator based on DC-to-DC converters and capacitor-diode voltage multipliers for water treatment applications," *IEEE Trans. Dielectrics Elect. Insul.*, vol. 22, no. 6, pp. 3290–3298, Dec. 2015.

[97] A. A. Elserougi, M. Faiter, A. M. Massoud, and S. Ahmed, "A transformerless bipolar/unipolar high-voltage pulse generator with low-voltage components for water treatment applications," *IEEE Trans. Ind. Appl.*, vol. 53, no. 3, pp. 2307–2319, May 2017.

[98] A. Darwish, M. A. Elgenedy, S. J. Finney, B. W. Williams, and J. R. McDonald, "A step-up modular high-voltage pulse generator based on isolated input-parallel/output-series voltage-boosting modules and modular multilevel submodules," *IEEE Trans. Ind. Electron.*, vol. 66, no. 3, pp. 2207–2216, Mar. 2019.

[99] Z. Deng, Q. Yuan, S. Shen, J. Yan, Y. Wang, and W. Ding, "High voltage nanosecond pulse generator based on avalanche transistor Marx bank circuit and linear transformer driver," *Rev. Sci. Instrum.*, vol. 92, no. 3, Mar. 2021, Art. no. 034715.

[100] M. R. Kazemi, T. Sugai, A. Tokuchi, and W. Jiang, "Study of pulsed atmospheric discharge using solid-state LTD," *IEEE Trans. Plasma Sci.*, vol. 45, no. 8, pp. 2323–2327, Aug. 2017.

[101] Y. Feng, T. Sugai, and W. Jiang, "Solid-state bipolar linear transformer driver using inductive energy storage," *IEEE Trans. Plasma Sci.*, vol. 49, no. 9, pp. 2887–2892, Sep. 2021.

[102] Y. Mi, N. Xu, J. Chen, and Z. Li, "High-frequency bipolar solid-state LTD based on a self-triggering H-bridge," *IEEE Trans. Power Electron.*, vol. 37, no. 5, pp. 5898–5907, May 2022.

[103] W. Jiang, H. Sugiyama, and A. Tokuchi, "Pulsed power generation by solid-state LTD," *IEEE Trans. Plasma Sci.*, vol. 42, no. 11, pp. 3603–3608, Nov. 2014.

[104] M. A. Elgenedy, A. Darwish, S. Ahmed, and B. W. Williams, "A transition arm modular multilevel universal pulse-waveform generator for electroporation applications," *IEEE Trans. Power Electron.*, vol. 32, no. 12, pp. 8979–8991, Dec. 2017.

[105] S. Jiang, J. Wang, Y. Wang, Z. Li, and J. Rao, "A multilevel pulse generator based on series capacitor structure for cell electroporation," *IEEE Trans. Plasma Sci.*, vol. 48, no. 12, pp. 4235–4241, Dec. 2020.

[106] M. Gundersen, P. T. Vernier, S. B. Cronin, and S. Kerketta, "A review of diverse academic research in nanosecond pulsed power and plasma science," *IEEE Trans. Plasma Sci.*, vol. 48, no. 4, pp. 742–748, Apr. 2020.

[107] A. A. Elserougi, A. M. Massoud, and S. Ahmed, "A modular high-voltage pulse-generator with sequential charging for water treatment applications," *IEEE Trans. Ind. Electron.*, vol. 63, no. 12, pp. 7898–7907, Dec. 2016.

[108] L. M. Redondo, M. Zahyka, and A. Kandratsyeu, "Solid-state generation of high-frequency burst of bipolar pulses for medical applications," *IEEE Trans. Plasma Sci.*, vol. 47, no. 8, pp. 4091–4095, Aug. 2019.

[109] T. Matsumoto, D. Wang, T. Namihira, and H. Akiyama, "Energy efficiency improvement of nitric oxide treatment using nanosecond pulsed discharge," *IEEE Trans. Plasma Sci.*, vol. 38, no. 10, pp. 2639–2643, Oct. 2010.

[110] S. Y. Tseng, T. F. Wu, and M. W. Wu, "Bipolar narrow-pulse generator with energy-recovery feature for liquid-food sterilization," *IEEE Trans. Ind. Electron.*, vol. 55, no. 1, pp. 123–132, Jan. 2008.

[111] S. M. Starikovskaia, "Plasma-assisted ignition and combustion: Nanosecond discharges and development of kinetic mechanisms," *J. Phys. D: Appl. Phys.*, vol. 47, no. 35, Aug. 2014, Art. no. 353001.

[112] Y. Zhou et al., "Fast-rise-time trigger source based on solid-state switch and pulse transformer for triggered vacuum switch," *IEEE Trans. Dielectrics Elect. Insul.*, vol. 24, no. 4, pp. 2105–2114, Apr. 2017.

[113] S. M. Park and H. J. Ryoo, "Pulsed power modulator with active pull-down using diode reverse recovery time," *IEEE Trans. Power Electron.*, vol. 35, no. 3, pp. 2943–2949, Mar. 2020.

[114] BEHLKE, "HIGH voltage push-pull switching units." Accessed: Dec 13, 2023. [Online]. Available: https://www.behlke.com/pdf/ghts.pdf

[115] BEHLKE, "FSWP high-voltage push-pull pulser." Accessed: Dec 13, 2023. [Online]. Available: https://www.behlke.com/pdf/fswp 91-01_rs.pdf

[116] PULSE, "Rectangular wave HVPG." Accessed: Dec 13, 2023. [Online]. Available: http://pulse-technology.cn/html/202009/94.html

[117] PULSE, "Adjustable parameters HVPG." Accessed: Dec 13, 2023. [Online]. Available: http://pulse-technology.cn/html/202010/96.html

[118] N. S. H. Voltage, "Spark gap trigger systems." Accessed: Dec 13, 2023. [Online]. Available: https://www.highvoltageprobes.com/wp-content/uploads/2019/11/Trigger55kVBrochure110517.pdf

[119] S. Technologies, "Standard 10 kV pulser." Accessed: Dec 13, 2023. [Online]. Available: https://sydortechnologies.com/pulse-generators/standard-10-kv-pulser/

[120] BNC, "±6 kV pulse output bipolar pulse generator." Accessed: Dec 13, 2023. [Online]. Available: https://www.berkeleynucleonics.com/sites/default/files/products/resources/pvx-4130_bnc_datasheet.pdf
[121] EMC, "High-voltage impulse generator." Accessed: Dec 13, 2023. [Online]. Available: https://absolute-emc.com/uploads/files/1584386077_PG20e4k.pdf
[122] HPPI. "120 A high voltage pulse generator," Accessed: Dec 13, 2023. [Online]. Available: https://www.hppi.de/files/TLP12010C.pdf
[123] S. R. Jang, C. H. Yu, and H. J. Ryoo, "Simplified design of a solid state pulsed power modulator based on power cell structure," *IEEE Trans. Ind. Electron.*, vol. 65, no. 3, pp. 2112–2121, Mar. 2018.
[124] J.-S. Bae et al., "Compact solid-state Marx modulator with fast switching for nanosecond pulse," *IEEE Trans. Power Electron.*, vol. 37, no. 8, pp. 9406–9414, Aug. 2022.
[125] T. Yin, L. Lin, C. Xu, D. Zhu, and K. Jing, "A hybrid modular multilevel converter comprising SiC MOSFET and Si IGBT with its specialized modulation and voltage balancing scheme," *IEEE Trans. Ind. Electron.*, vol. 69, no. 11, pp. 11272–11282, Nov. 2022.
[126] Q.-X. Guan et al., "An extremely high efficient three-level active neutral-point-clamped converter comprising SiC and Si hybrid power stages," *IEEE Trans. Power Electron.*, vol. 33, no. 10, pp. 8341–8352, Oct. 2018.
[127] J. Wang, H. S. H. Chung, and R. T. H. Li, "Characterization and experimental assessment of the effects of parasitic elements on the MOSFET switching performance," *IEEE Trans. Power Electron.*, vol. 28, no. 1, pp. 573–590, Jan. 2013.
[128] L. Collier, T. Kajiwara, J. Dickens, J. Mankowski, and A. Neuber, "Fast SiC switching limits for pulsed power applications," *IEEE Trans. Plasma Sci.*, vol. 47, no. 12, pp. 5306–5313, Dec. 2019.
[129] E. Laloya, Ó. Lucía, H. Sarnago, and J. M. Burdío, "Heat management in power converters: From state of the art to future ultrahigh efficiency systems," *IEEE Trans. Power Electron.*, vol. 31, no. 11, pp. 7896–7908, Nov. 2016.
[130] C. H. Van Der Broeck, R. D. Lorenz, and R. W. De Doncker, "Monitoring 3-D temperature distributions and device losses in power electronic modules," *IEEE Trans. Power Electron.*, vol. 34, no. 8, pp. 7983–7995, Aug. 2019.
[131] M. Fernandez, X. Perpina, M. Vellvehi, O. Avino-Salvado, S. Llorente, and X. Jorda, "Power losses and current distribution studies by infrared thermal imaging in soft- and hard-switched IGBTs under resonant load," *IEEE Trans. Power Electron.*, vol. 35, no. 5, pp. 5221–5237, May 2020.
[132] E. Imaz, R. Alonso, C. Heras, I. Salinas, E. Carretero, and C. Carretero, "Infrared thermometry system for temperature measurement in induction heating appliances," *IEEE Trans. Ind. Electron.*, vol. 61, no. 5, pp. 2622–2630, May 2014.
[133] J. C. Olivares-Galvan, S. Magdaleno-Adame, R. Escarela-Perez, R. Ocon-Valdez, P. S. Georgilakis, and G. Loizos, "Reduction of stray losses in flange–bolt regions of large power transformer tanks," *IEEE Trans. Ind. Electron.*, vol. 61, no. 8, pp. 4455–4463, Aug. 2014.
[134] D. Rothmund, D. Bortis, and J. W. Kolar, "Accurate transient calorimetric measurement of soft-switching losses of 10-kV SiC MOSFETs and diodes," *IEEE Trans. Power Electron.*, vol. 33, no. 6, pp. 5240–5250, Jun. 2018.
[135] J. Jörg, S. Taraborrelli, G. Sarriegui, R. W. De Doncker, R. Kneer, and W. Rohlfs, "Direct single impinging jet cooling of a MOSFET power electronic module," *IEEE Trans. Power Electron.*, vol. 33, no. 5, pp. 4224–4237, May 2018.
[136] K. Gould, S. Q. Cai, C. Neft, and A. Bhunia, "Liquid jet impingement cooling of a silicon carbide power conversion module for vehicle applications," *IEEE Trans. Power Electron.*, vol. 30, no. 6, pp. 2975–2984, Jun. 2015.
[137] C. M. Barnes and P. E. Tuma, "Practical considerations relating to immersion cooling of power electronics in traction systems," *IEEE Trans. Power Electron.*, vol. 25, no. 9, pp. 2478–2485, Sep. 2010.
[138] I. Aranzabal, I. M. De Alegria, N. Delmonte, P. Cova, and I. Kortabarria, "Comparison of the heat transfer capabilities of conventional single- and two-phase cooling systems for an electric vehicle IGBT power module," *IEEE Trans. Power Electron.*, vol. 34, no. 5, pp. 4185–4194, May 2019.
[139] Y. Wang, L. Ren, Z. Yang, Z. Deng, and W. Ding, "Application of two-phase immersion cooling technique for performance improvement of high power and high repetition avalanche transistorized subnanosecond pulse generators," *IEEE Trans. Power Electron.*, vol. 37, no. 3, pp. 3024–3039, Mar. 2022.
[140] Y. Ko, V. Raveendran, M. Andresen, and M. Liserre, "Advanced discontinuous modulation for thermally compensated modular smart transformers," *IEEE Trans. Power Electron.*, vol. 35, no. 3, pp. 2445–2457, Mar. 2020.
[141] J. Sheng et al., "Active thermal control for hybrid modular multilevel converter under overmodulation operation," *IEEE Trans. Power Electron.*, vol. 35, no. 4, pp. 4242–4255, Apr. 2020.
[142] R. Han et al., "Thermal stress balancing oriented model predictive control of modular multilevel switching power amplifier," *IEEE Trans. Ind. Electron.*, vol. 67, no. 11, pp. 9028–9038, Nov. 2020.
[143] J. Kuprat, C. H. Van Der Broeck, M. Andresen, S. Kalker, M. Liserre, and R. W. De Doncker, "Research on active thermal control: Actual status and future trends," *IEEE J. Emerg. Sel. Topics. Power Electron.*, vol. 9, no. 6, pp. 6494–6506, Dec. 2021.
[144] S. Falun et al., "Research progress on miniaturization of high power repetition frequency Marx type pulse power source," *High Power Laser Part. Beams*, vol. 30, no. 2, Feb. 2018, Art, no. 020201.
[145] C. Li et al., "Design and development of a compact all-solid-state high-frequency picosecond-pulse generator," *IEEE Trans. Plasma Sci.*, vol. 46, no. 10, pp. 3249–3256, Oct. 2018.
[146] S. R. Jang, C. H. Yu, and H. J. Ryoo, "Trapezoidal approximation of LCC resonant converter and design of a multistage capacitor charger for a solid-state Marx modulator," *IEEE Trans. Power Electron.*, vol. 33, no. 5, pp. 3816–3825, May 2018.

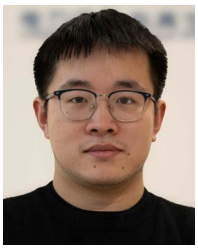

YINGJIAN ZHUGE (Student Member, IEEE) received the B.S. degree in electrical engineering from Zhejiang University, Hangzhou, China, in 2021. He is currently working toward the Ph.D. degree in electrical engineering with the School of Information Science and Technology, ShanghaiTech University, Shanghai, China. His research interests include pulsed power technology, and high-voltage pulse generators.

JUNRUI LIANG (Senior Member, IEEE) received the Ph.D. degree in mechanical and automation engineering from The Chinese University of Hong Kong (CUHK), Hong Kong, in 2010. Since November 2013, he has been with the School of Information Science and Technology, ShanghaiTech University, Shanghai, China, as an Assistant Professor. His most significant contribution was that he extended the impedance modeling and analysis, which conventionally was only used for linear systems, to some nonlinear power conversion systems, such as the class-E power amplifier and piezoelectric energy harvesting systems. His recent research interests include dynamics of nonlinear electromechanical coupling systems, kinetic energy harvesting and vibration control, electrical power conversion and utilization research, and renewable energy.

MINFAN FU (Senior Member, IEEE) received the B.S., M.S., and Ph.D. degrees in electrical and computer engineering from the University of Michigan Shanghai Jiao Tong University Joint Institute, Shanghai Jiao Tong University, Shanghai, China, in 2010, 2013, and 2016, respectively. From 2016 to 2018, he held a postdoctoral position with the Center for Power Electronics Systems (CPES), Virginia Polytechnic Institute and State University, Blacksburg, VA, USA. He is currently an Assistant Professor with the School of Information Science and Technology, ShanghaiTech University, Shanghai, China. His research interests include megahertz wireless power transfer, high-frequency power conversion, high-frequency magnetic design, and application of wide bandgap devices. He holds one U.S. patent, seven Chinese patents, and has authored or coauthored more than 80 papers in prestigious IEEE journals and conferences.

TENG LONG (Member, IEEE) received the B.Eng. degree in electrical engineering from the Huazhong University of Science and Technology, Wuhan, China, the B.Eng. (first-class Hons.) degree in electrical engineering from the University of Birmingham, Birmingham, U.K., in 2009, and the Ph.D. degree in engineering from the University of Cambridge, Cambridge, U.K., in 2013. Until 2016, he was a Power Electronics Engineer with the General Electric Power Conversion business, Rugby, U.K. He is currently a Full Professor with the University of Cambridge. He is a Chartered Engineer (CEng) registered with the Engineering Council in the U.K. His research interests include power electronics, electrical machines, and machine drives.

HAOYU WANG (Senior Member, IEEE) received the bachelor's degree with distinguished honor in electrical engineering from Zhejiang University, Hangzhou, China, and the master's and Ph.D. degrees in electrical engineering from the University of Maryland, College Park, MD, USA. In September 2014, he joined the School of Information Science and Technology, where he is currently an Associate Professor with tenure. In 2023, he visited the University of Cambridge as a Visiting Academic Fellow. His research interests include power electronics, pulsed power supply, plug-in electric vehicles, and renewable energy systems. Dr. Wang is an Associate Editor for IEEE TRANSACTIONS ON INDUSTRIAL ELECTRONICS, IEEE TRANSACTIONS ON TRANSPORTATION ELECTRIFICATION, and *CPSS Transactions on Power Electronics and Applications*. He is also a Guest Editor for IEEE JOURNAL OF EMERGING AND SELECTED TOPICS IN POWER ELECTRONICS.